National Library of Canada
Canadian Theses Service
Ottawa, Canada
K1A 0N4

Bibliothèque nationale du Canada
Services des thèses canadiennes

CANADIAN THESES

THÈSES CANADIENNES

NOTICE

The quality of this microfiche is heavily dependent upon the quality of the original thesis submitted for microfilming. Every effort has been made to ensure the highest quality of reproduction possible.

If pages are missing, contact the university which granted the degree.

Some pages may have indistinct print especially if the original pages were typed with a poor typewriter ribbon or if the university sent us an inferior photocopy.

Previously copyrighted materials (journal articles, published tests, etc.) are not filmed.

Reproduction in full or in part of this film is governed by the Canadian Copyright Act, R.S.C. 1970, c. C-30.

AVIS

La qualité de cette microfiche dépend grandement de la qualité de la thèse soumise au microfilmage. Nous avons tout fait pour assurer une qualité supérieure de reproduction.

S'il manque des pages, veuillez communiquer avec l'université qui a conféré le grade.

La qualité d'impression de certaines pages peut laisser à désirer, surtout si les pages originales ont été dactylographiées à l'aide d'un ruban usé ou si l'université nous a fait parvenir une photocopie de qualité inférieure.

Les documents qui font déjà l'objet d'un droit d'auteur (articles de revue, examens publiés, etc.) ne sont pas microfilmés.

La reproduction, même partielle, de ce microfilm est soumise à la Loi canadienne sur le droit d'auteur, SRC 1970, c. C-30.

THIS DISSERTATION HAS BEEN MICROFILMED EXACTLY AS RECEIVED

LA THÈSE A ÉTÉ MICROFILMÉE TELLE QUE NOUS L'AVONS REÇUE

Canada

NL-339 (r. 86/06)

THE UNIVERSITY OF ALBERTA

ANALYSIS OF SEISMIC INSTABILITY OF THE VANCOUVER ISLAND LITHOPROBE TRANSECT

by

Li Qing

A THESIS

SUBMITTED TO THE FACULTY OF GRADUATE STUDIES AND RESEARCH

IN PARTIAL FULFILMENT OF THE REQUIREMENTS FOR THE DEGREE

OF Master of Science

IN

Geophysics

Department of Physics

Edmonton, Alberta

Spring 1986

Permission has been granted to the National Library of Canada to microfilm this thesis and to lend or sell copies of the film.

The author (copyright owner) has reserved other publication rights, and neither the thesis nor extensive extracts from it may be printed or otherwise reproduced without his/her written permission.

L'autorisation a été accordée à la Bibliothèque nationale du Canada de microfilmer cette thèse et de prêter ou de vendre des exemplaires du film.

L'auteur (titulaire du droit d'auteur) se réserve les autres droits de publication; ni la thèse ni de longs extraits de celle-ci ne doivent être imprimés ou autrement reproduits sans son autorisation écrite.

ISBN 0-315-30270-4

THE UNIVERSITY OF ALBERTA

RELEASE FORM

NAME OF AUTHOR Li Qing

TITLE OF THESIS ANALYSIS OF SEISMIC INSTABILITY OF THE VANCOUVER ISLAND LITHOPROBE TRANSECT

DEGREE FOR WHICH THESIS WAS PRESENTED Master of Science

YEAR THIS DEGREE GRANTED Spring 1986

Permission is hereby granted to THE UNIVERSITY OF ALBERTA LIBRARY to reproduce single copies of this thesis and to lend or sell such copies for private, scholarly or scientific research purposes only.

The author reserves other publication rights, and neither the thesis nor extensive extracts from it may be printed or otherwise reproduced without the author's written permission.

(SIGNED) Qing Li

PERMANENT ADDRESS:

Institute of Geophysics

S.S.B. Beijing

P.R. China

DATED Dec 5 1985

THE UNIVERSITY OF ALBERTA

FACULTY OF GRADUATE STUDIES AND RESEARCH

The undersigned certify that they have read, and recommend to the Faculty of Graduate Studies and Research, for acceptance, a thesis entitled ANALYSIS OF SEISMIC INSTABILITY OF THE VANCOUVER ISLAND LITHOPROBE TRANSECT submitted by Li Qing in partial fulfilment of the requirements for the degree of Master of Science in Geophysics.

.....

Supervisor

.....

.....

.....

Date..... December 6, 1985

Abstract

Using the results of seismic refraction and reflection surveys and gravity measurement in the Vancouver Island region a finite element model has been built for that region. Stress estimates are obtained from this model and have been combined with rock failure criteria to yield measures of seismic risk in terms of probability. These measures allow the study of geodynamic processes in such a way that the observed seismicity can be linked to a tectonic driving mechanism.

A seismic instability function was constructed using the theory of a Griffith crack. This function depends on the distribution of cracks within the body and the mechanical properties of the materials. The measure of the seismically unstable zone using the instability function is better than measure using the stress directly.

The results obtained from the instability analysis for the Vancouver Island region are in agreement with the observed seismicity and lead to the suggestion that the driving mechanism of the oceanic plate of the Vancouver Island subduction region is provided by gravitational ridge push and mantle convection. The interaction between the oceanic plate and continental plate is one of main reasons for the seismicity in the region beneath Vancouver Island.

Acknowledgements

I would like to express my gratitude to my supervisor Dr. Edo Nyland for his patience, guidance and gentle prods throughout the course of the study. I would also like to thank Dr. Nyland for his suggestion on my future study.

I take this opportunity to thank Dr. Antonio Uribe for his help during my first year of study here and his valuable suggestions for my work.

I would like to thank Dr. Xuanzhi Wu and all my colleagues for many useful discussions and many good times.

I am grateful to Dr. Zheng Rongsheng, Ms. Shong Zhaoyi and Dr. Feng Rui at Institute of Geophysics of State Seismological Bureau at Beijing for their support during my study here.

Without the generous support of the Department of Physics at University of Alberta in the form of teaching assistantships this work would not have been possible. The excellent computing facilities of the University of Alberta are invaluable in this study.

Last but not least, I would thank my wife Jing and my parents for their unconditional support thoughout my study.

Table of Contents

Chapter — Page

I. Introduction 1

1.1 Geological Environment of Vancouver Island 2

1.2 Plate Tectonic Regime of the Coast of Western Canada 7

1.3 Seismic Structure of Vancouver Island ... 13

1.4 Tectonic Stress related Earthquake Phenomena 23

1.5 Earthquake Activity in the Vancouver Island Region 25

II. The Model of Vancouver Island Subducting Lithosphere 29

2.1 The Finite Element Model and Boundary Conditions 34

III. Analysis of Stress State and Instability 47

3.1 The Concept of Stability 47

3.2 Instability Analysis for Vancouver Island Region 56

IV. Conclusions 68

References 73

Appendix 77

List of Table Captions

Table page

Table 1 — Spreading parameters for Juan de Fuca and Explorer Ridges averaged over 1 million year intervals. After Riddihough 1977. 10

Table 2 — Parameters of the model.....38

Table 3 — Thermodynamic Efficiency and Power of Core and Mantle Convection. After Stacey 1977.....41

List of Figure Captions

Figure Page

1 shows the outline map of Cordilleran Belts, modified from Muller 1977.....3

2 (a) shows evolution of the Cordilleran Belts, (b) shows geologic history of three structural units of Vancouver Island, modified from Muller 1977.....4

3 The tectonic map of western Canada showing the main lithosphere plate boundaries and relative plate motion.8

4 shows the interaction vectors for Juan de Fuca and Explorer plates relative to American plate, modified from Riddihough 1977.....12

5 shows Bouguer gravity and gravity model cross-section across southern Vancouver Island. The small solid rectangles are the seismic control. Modified from Riddihough 1979.....14

6 shows the locations of seismic lines in VISP 1980 denoted by ——, and the Lithoprobe seismic profiles denoted by ---.....15

7 (a) shows the suggested three models corresponding to the left end of (b). (b) shows two-dimensional velocity distribution along the profile shown in Figure 6..After McMechan and Spence 1983.....17

8 shows two dimensional structure determined by ray tracing technique. Insert (a) shows velocity - depth models at location A (solid line) and B (dashed line); insert (b) at location OBS1. Modified from Ellis 1983.....18

9 shows the preliminary interpretation of Lithoprobe VISP1. Modified from Yorath at el 1985.....21

10 shows the velocity model and tectonic cross-section across the continental margin. Modified from Yorath et al. 1985.....22

11 shows the earthquake epicentres of the western Canadian margin. The area in the rectangle is studied in this thesis.....26

12 shows the distribution of the foci of the earthquakes within the rectangle in Figure 11.....27

13 shows the distribution of dimensionless temperature T' in a subducting plate. Modified from McKenzie 1969.33

14 shows Stacey's heat engine for mantle convection. The path A→B and C→D are adiabatic processes, path B→C and D→A isobaric processes. Modified from Stacey 1977.....40

15 shows the nodal distribution and the structure of the finite element model. The commands on top are used for modifying the model; see Appendix.....46

16 shows the general definition of instability as the minimum distance from the surface of the Mohr circle to the failure criterion.....49

17 shows the assumed distribution of cracks in a body. $P_o(c)$ is calculated for σ=0.1.....54

18 shows the probability function of P, which is calculated for $\lambda^2/\sigma^2=7\times10^8$, n=100.....57

19 (a) shows the average stress distribution and (b) the maximum shear stress distribution of the gravitational model.....59

20 shows the distribution of instability for the model under the gravitational load.....60

21 shows the instability distribution for the model

with ridge push force exerted on oceanic plate.....62

22 shows the distribution of instability for the model with an active viscous drag on the bottom of oceanic plate by the asthenosphere.....64

I. Introduction

An earthquake can be thought of as a sudden failure of rock when it is unable to support an increase of stress. Therefore, regional stress distribution and mechanical properties of rocks are directly related to the earthquake. The plate tectonic hypothesis gives an explanation of global seismic activity along the world's major seismic belts. Seismic observations show that most earthquakes happen on the edges of the plates and are governed by the distribution of the stress within the lithosphere. Stress distribution modelling on the boundaries of plates is thus important in studying the state of the stress, and it can give a quantitative view of the geodynamic processes of an area.

A subduction zone is the interplate boundary where an oceanic plate collides with a continental plate and the denser oceanic plate subducts beneath the continental one. It is a zone of concentration of stress because it contains discontinuities in the lithosphere. Many geophysical phenomena are related closely to the subducted plate, which plays an important role leading to the relations between many different geophysical processes occurring in the interior of the earth.

The margin of British Columbia is an active zone with very complex geological processes. The results of seismic experiments and the interpretation of gravity data on Vancouver Island strongly suggest that it is a subduction zone area. It is the purpose of this thesis to analyze the

distribution of stress in the subduction zone with a finite element model. This will suggest possible relations between seismicity and the distribution of the instability which measures the risk of seismicity in the model, and increase understanding of the geodynamic behaviour of Vancouver Island.

1.1 Geological Environment of Vancouver Island

In this section the geological environment of Vancouver Island is introduced based on the papers of J. E. Muller, 1977 and J. W. H. Monger et al., 1972.

The Canadian Cordillera has been divided into several longitudinal physiographic and tectonic belts (Figure 1, Muller 1977, Monger 1972). From west to east they are (1) sedimentary, "miogeosynclinal" strata in the Rocky Mountains Belt, (2) metamorphic and granitic rocks in the Omineca Crystalline Belt, (3) mainly unmetamorphosed and low-grade sedimentary and volcanic "eugeosynclinal" and "epieugeosynclinal" strata in the Intermontane Belt, (4) predominantly granitic rock in the Coast Range Plutonic Complex, (5) largely unmetamorphosed and low-grade sedimentary and volcanic "eugeosynclinal" strata in the Insular Belt, (6) Inner Pacific Belt and (7) Outer Pacific Belt which are defined by Muller (1977).

The distribution in time and space of various lithological units of Cordilleran Belts are shown in Figure 2 (Muller 1977, Monger 1972). The space between vertical

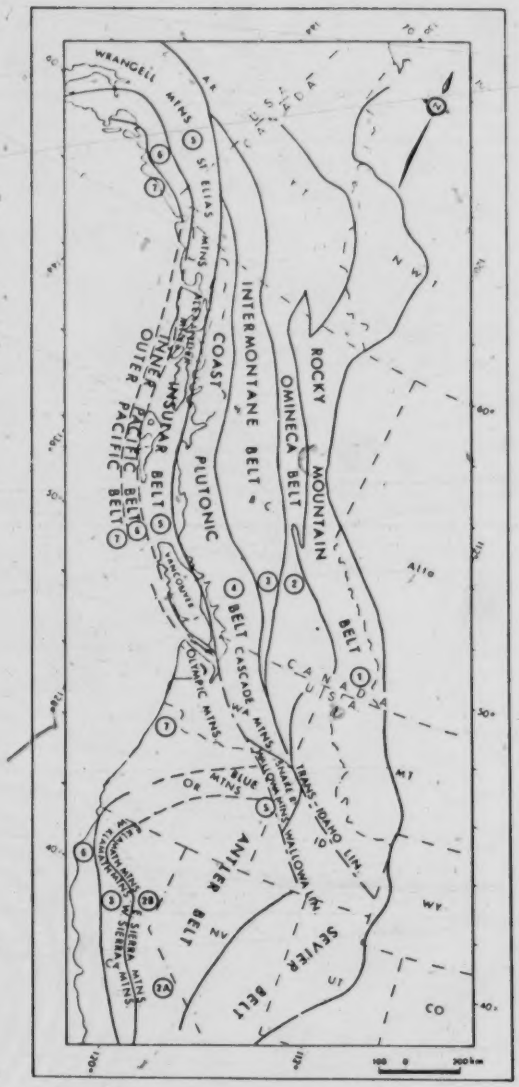

Figure 1.... shows the outline map of Cordilleran Belts, modified from Muller 1977.

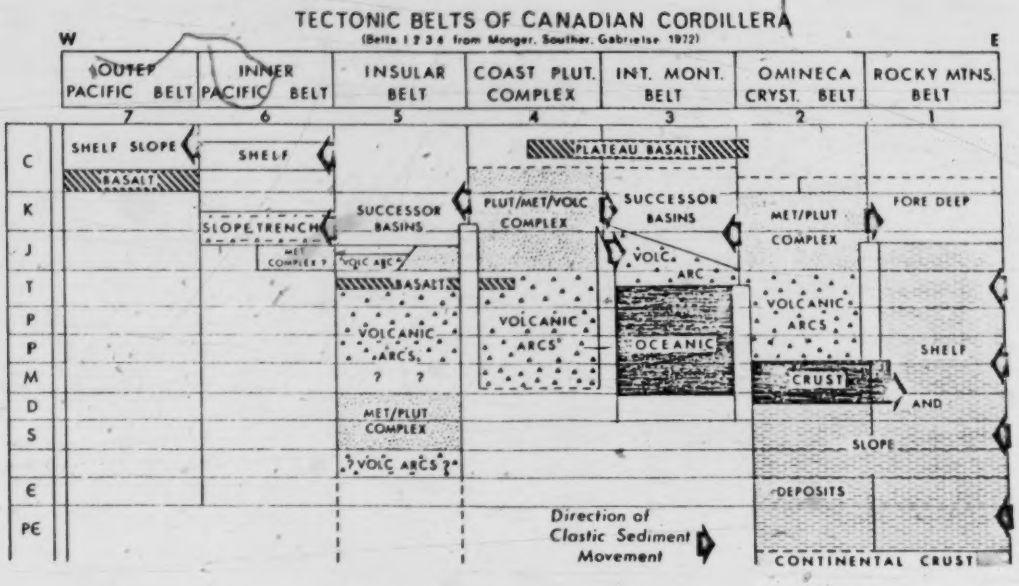

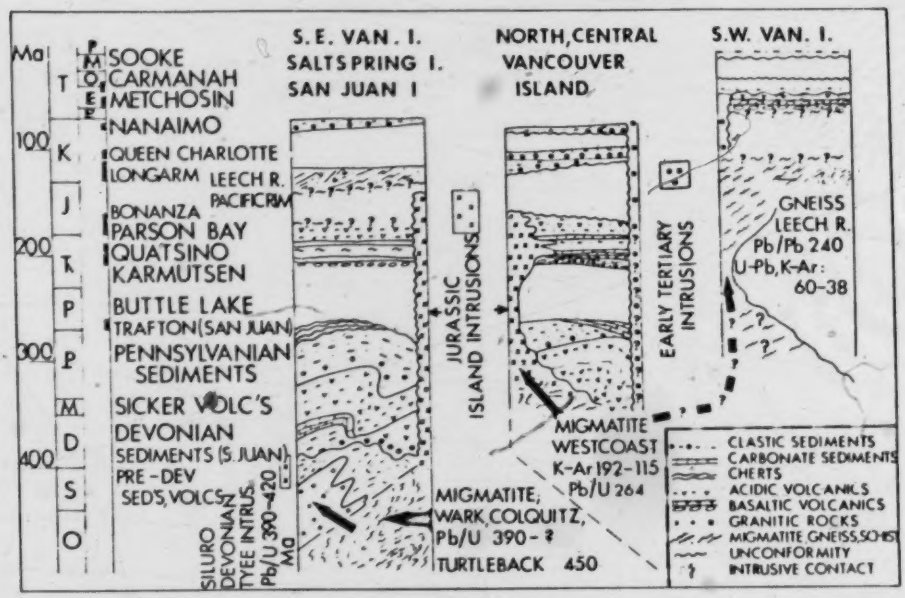

Figure 2.... (a) shows evolution of the Cordilleran Belts, (b) shows geologic history of three structural units of Vancouver Island, modified from Muller 1977.

columns indicates that no linkages are known between the belts. These linkages, which take the form of detritus of clastics shed from one belt to another, are stratigraphic units spanning two contiguous belts. The arrows indicate the direction of clastic movement.

Vancouver Island is a part of the Insular Belt. It is made up of Paleozoic, Mesozoic and Cenozoic volcanic, plutonic, sedimentary and metamorphic rocks. The Island's oldest rocks are the Sicker Group which formed in Paleozoic time, and are dominated by epiclastic strata with lesser amounts of volcanic and pyroclastic rocks. The main stratigraphic and structural unit is the Karmutsen Formation, a thick, Upper Triassic shield of relatively uniform basaltic lava that separates middle and upper Paleozoic from Jurassic and younger volcanic, sedimentary and plutonic units (Muller 1977, Yorath et al 1984).

The geologic history of the main part of Vancouver Island is summarized in the middle column of Figure 2b (Muller 1977). Those parts that are considered extensions of the Cascade and Olympic Mountains are shown in the right and left column respectively. On the southeast tip of the Island, gneisses of diorite and granodioritic composition of early Paleozoic form the basement underlying Sicker Group rock which were intruded at the Devonian or older (Left column in Figure 2b). The Tyee Intrusions at Maple Bay, which are located at the south end of the Island, are schistose quartz porphyrys that intrude tuff and uralite

porphyry with typical lithology of Paleozoic Sicker Group volcanics. They are probably Pennsylvanian in age, but another explanation, thier being Jurassic in age, is also possible. The lower part of the Sicker Group consists of breccia, tuff, and flows of basaltic to rhyolitic composition. The Buttle Lake Formation is the uppermost part of the Sicker Group and consists of limestone with scarce to abundant interbedded chert, and is up to 2500ft thick (Yole 1969). On the west side of Orcas Island a conglomerate with argillite, chert, volcanic, and limestone clasts lacks granitoid clasts.

The early Mesozoic stratigraphy of the Island Mountains is represented by Middle Triassic to Lower Jurassic volcanic and sedimentary rocks and lower to Middle Jurassic Island Intrusions. Tholeiitic basalts of the Karmutsen Formation, in a general upward succession of pillow lavas, breccias, and flows up to 6000m thick, form the bulk of the rocks underlying central Vancouver Island.

The Pacific Rim Complex, an assemblage of greywacke, argillite, chert and greenstone, and Leech River sediments, which are schistose greywacke and argillite, is considered to be lower slope, trench, and oceanic deposits. The Early Cretaceous shelf sequence of the west coast is succeeded by the Upper Cretaceous Nanaimo Group of eastern Vancouver Island. (Muller 1977).

1.2 Plate Tectonic Regime of the Coast of Western Canada

In this section the plate tectonic regime of the coast of western Canada is discussed mainly based on the papers of R. P. Riddihough, 1977 and C. E. Keen and R. D. Hyndman, 1979.

The tectonic regime of the continental margin of western Canada is dominated by the relation of three main lithospheric plates: the Pacific plate, the America plate and the Juan de Fuca plate (Keen and Hyndman, 1979). Figure 3 shows the tectonic map of western Canada. The small northern part of the Juan de Fuca plate has been named the Explorer plate, It is active and moves independently. The boundary between the Pacific and America plates is defined by the Queen Charlotte transform fault, which lies along the edge of the continental shelf from southern edge of the Queen Charlotte Islands to southern Alaska; the motion on the fault is right lateral at about 5.5 cm/yr. The boundary between the Explorer-Pacific plates and the Juan de Fuca-Pacific plates is defined by numerous en-echelon spreading axes, offset by short transform segments. The present rate of the motion across this boundary ranges from about 4 to 6 cm/yr (full spreading rate). The boundary between the Juan de Fuca and Explorer plates is known as the Nootka fracture zone, which is a strike slip fault with a left lateral motion of about 2 cm/yr, extending northeasterly from the north end of the Juan de Fuca ridge to the continental shelf off north central Vancourver Isand.

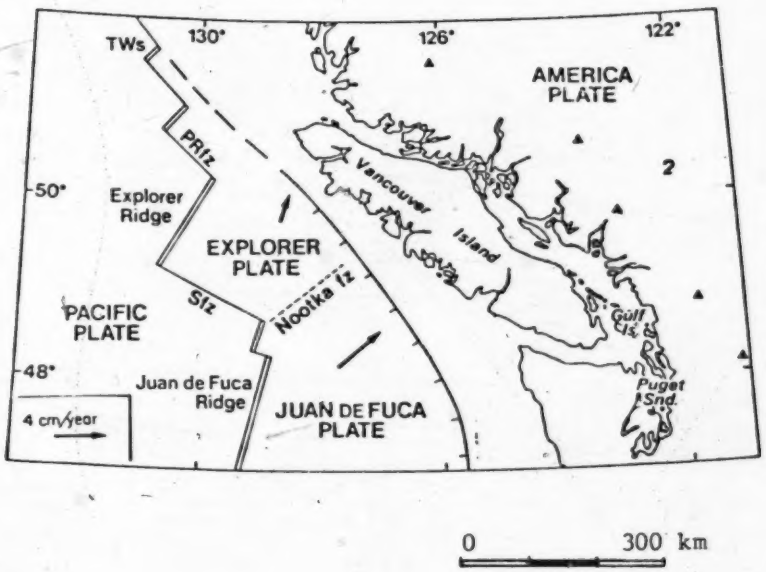

Figure 3.... The tectonic map of western Canada showing the main lithosphere plate boundaries and relative plate motion.

The boundary between the America plate and the Juan de Fuca and Explorer plates is a zone of convergence or subduction, with underthrusting probably starting near the base of the continental slope with rates from 1 to 3cm/yr (Keen and Hyndman, 1979).

That subduction has occurred on the boundaries between the Juan de Fuca, Explorer and American plates in the past few million years is well established. Doubts as to whether it is continuing at present arise primarily from the lack of a deep margin trench, from lack of deep earthquakes in a Wadati-Benioff zone and of a thrust mechanism beneath the continental slope and shelf. Riddihough and Hyndman (1976) have concluded from a study of geological and geophysical data that the subduction continues to the present. Sediment compression, uplift and folding at the base of the slope also indicate the subduction is almost certainly taking place at present (Carson et al. 1974).

Riddihough (1977) gave a detailed examination of the spreading rate and direction of those plates under the assumption that the anomaly lineation azimuths measured from present magnetic anomaly maps have not been subjected to subsequent rotation and are therefore representative of the spreading direction when they were formed. The spreading parameters calculated for the Juan de Fuca and Explorer ridges for last 10 Ma years are shown in Table 1 (Riddihough 1977). A plate interaction vector is used to describe rate and direction of relative motion of plates. They were drawn

Table 1: Spreading parameters for the Juan de Fuca and Explorer Ridges averaged over 1 million year intervals.

Epoch Ma	Juan de Fuca Ridge				Explorer Ridge			
	West (Jw)		East (Je)		West (Ew)		East (Ee)	
	Rate	Direction	Rate	Direction	Rate	Direction	Rate	Direction
9.5	—	—	—	—	3.3	91°	—	—
8.5	3.3	91°	—	—	2.6	93°	—	—
7.5	3.5	91°	3.6	101°	2.6	93°	—	—
6.5	3.7	97°	3.6	99°	3.0	100°	—	—
5.5	3.4	97°	3.3	100°	2.8	99°	—	—
4.5	3.4	103°	3.4	104°	2.7	101°	—	—
3.5	3.0	111°	3.0	109°	3.2	107°	—	125°
2.5	3.2	110°	3.1	108°	2.7	121°	3.0	131°
1.5	3.0	108°	2.8	109°	—	124°	3.0	130°
0.5	3.1	110°	3.1	110°	2.1	126°	2.1	129°

*Spreading rates are half-rates in cm/yr. Spreading directions are orthogonal to magnetic anomaly azimuths measured from true North.

for the Juan de Fuca and Explorer plates relative to the American plate, and the relative motion between the Sovanco Fracture Zone (Figure 4). It is shown that the Juan de Fuca plate moved in a direction between N35°E and N50°E relative to the American plate for the last 9 million years. At present it moves in the direction of N35°E with a convergence rate of approximately 3.5cm/year. The rate deduced from sediment compression, uplift and folding at the base of the slope can give a minimum estimate of convergence rate. The values derived by Silver (1972) and Von Heune (1973) are lower than those calculated by Riddihough (Carson et al. 1974). The direction of motion of the Explorer plate relative to the American plate has changed from N38°E at 9.5Ma to N26°E at 3.5Ma, and then changed to N6°E at present. The convergence rate of the subduction at the Vancouver Island continental margin is 1.4cm/year during the last million years.

The Sovanco Fracture Zone was initiated between the Juan de Fuca and Explorer segments of the ridge as a result of the "break" of the ridge approximately 7 million years ago (Riddihough 1977). As the spreading rate of the western Explorer Ridge is less than that of the westen Juan de Fuca Ridge, the Explorer ridge migrated westward relative to the Juan de Fuca Ridge. The rotation of the Explorer Ridge implies compressional interaction at the Sovanco Fracture Zone. Such an interaction continued at least in the last 0.5 million years (Barr 1972). The relative motion between the

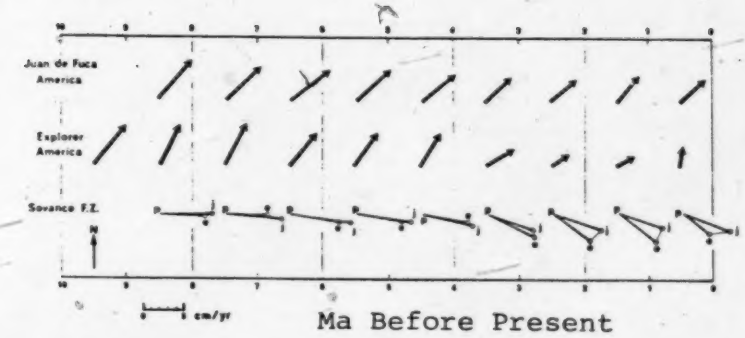

Figure 4.... shows the interaction vectors for Juan de Fuca and Explorer plates relative to American plate, modified from Riddihough 1977.

Explorer and Juan de Fuca plates could have been accommodated by the occurrence of a left lateral shear zone trending along the direction of the residual interaction vector EJ (see Figure 4). This is known as the Nootka Fault Zone which is clearly evident in the compilation of all earthquakes that are located in the area (Milne et al. 1978). Barr (1974) identified the fault trend from the northern end of the Juan de Fuca Ridge through 50°N, 125°W. The fault plane solutions from a number of large earthquakes are consistent with NE-SW left lateral strike slip motion. If we assume the fault initiated in conformity with EJ (see Figure 4) which is a relative movement vector, it would by now run beneath Vancouver Island in a NE direction through 50°N, 125°W (Riddihough 1977).

1.3 Seismic Structure of Vancouver Island

Riddihough first carried out detailed modeling of Vancouver Island based on the gravity data. His structure models cross the Island. Figure 5 shows Bouguer gravity and the gravity model cross-section across southern Vancouver Island. In his models some points at the depth of the Moho discontinuity are poorly constrained by seismic data (Ellis et al. 1983) because these seismic profiles were located at a significant distance from the models and in a different tectonic environment.

Recently some seismic surveys have been conducted in the Vancouver Island region. Figure 6 shows the locations of

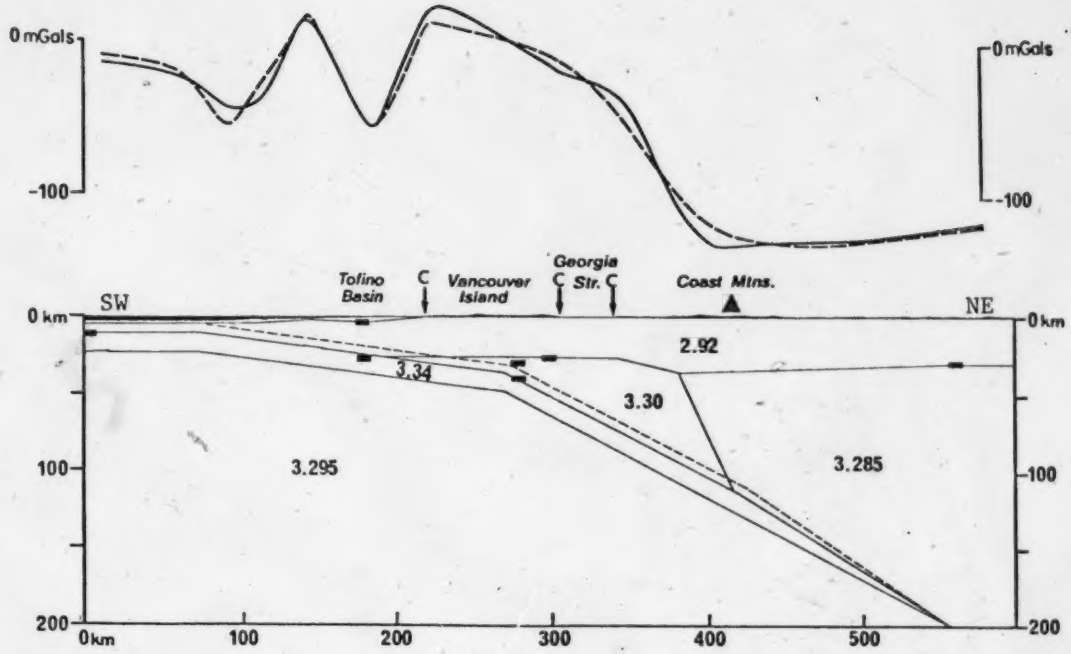

Figure 5.... shows Bouguer gravity and gravity model cross-section across southern Vancouver Island. The small solid rectangles are the seismic control. Modified from Riddihough 1979.

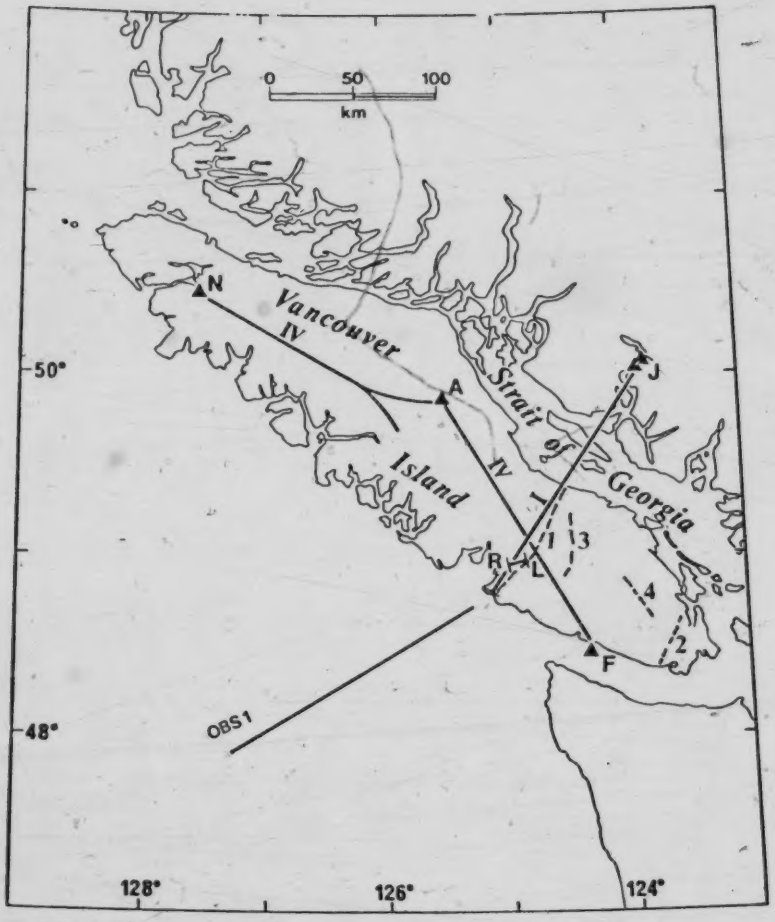

Figure 6.... shows the locations of seismic lines in VISP 1980 denoted by ——, and the Lithoprobe seismic profiles denoted by ---.

the refraction and reflection lines in Vancouver Island Seismic Project 1980 and four Lithoprobe seismic reflection profiles. By intepretation of these seismic data, the above gravity models were refined. McMechan and Spence (1983) analyzed the line IV along the axis of Vancouver Island and presented three laterally homogeneous models of crust and upper mantle (Figure 7). The upper 20 km of the structure is well constrained by the two reversed data profiles NA and AF. The structure of lower crust and upper mantle is only weakly constrained. Each of the 3 models fits certain travel-time and/or amplitude observations better than others. However, model 2 which contains a low velocity zone and a low upper mantle velocity of 7.5km/s at 37 km, is the preferred interpretation of McMechan and Spence. The actual structure may vary laterally, being nearer model 1 beneath the North half of Vancouver Island and nearer model 2 beneath the south.

The seismic profile line I was interpreted by Ellis et al (1983). The two dimensional model was determined by trial-and-error application of the ray tracing technique. The onshore-offshore line was studied with two shots at the end of the line and 17 shots over the profile. Figure 8 shows the resulting seismic velocity structure section. The two dimensional ray trace model, at the intersection with line IV, is constrained by the model of McMechan and Spence (1983), which contains a lowe. velocity zone in the low crust. The Moho west of the central portion of Vancouver

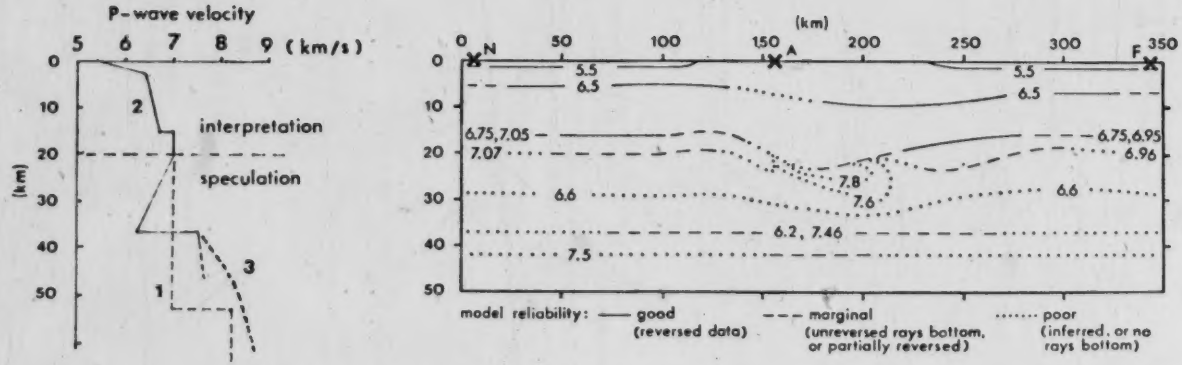

Figure 7.... (a)shows the suggested three models corresponding to the left end of (b). (b) shows two-dimensional velocity distribution along the profile shown in Figure 6. Modified from McMechan and Spence 1983.

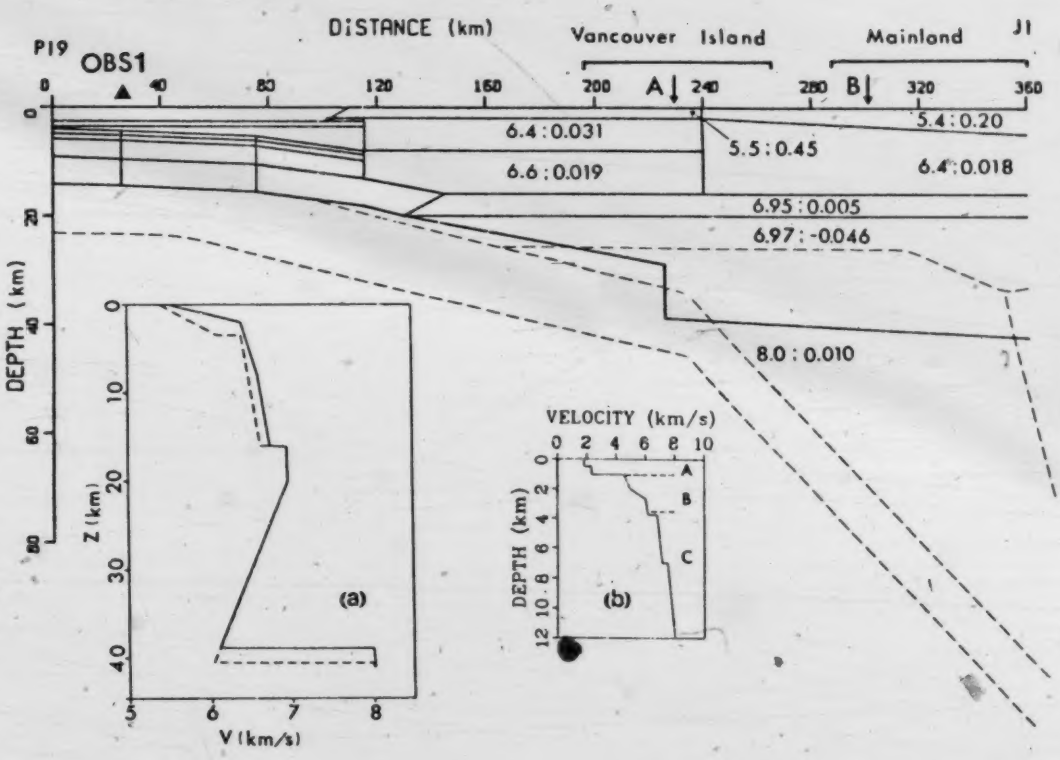

Figure 8.... shows two dimensional structure determined by ray tracing technique. Insert (a) shows velocity - depth models at location A (solid line) and B (dashed line); insert (b) at location OBS1. Modified from Ellis 1983.

Island appears to a dip near 6 degrees towards the continent, whereas that in the east is essentially flat-lying. This dip explains the difference between the west-to-east apparent velocity and the reversed east-to-west apparent velocity.

On the mainland the apparent velocities are almost the same in both directions and little dip is indicated. Comparing with the gravity models of Riddihough, the models are generally consistent west of the central portion of Vancouver Island. The position at which the continental crust suddenly thickens beneath the central part of Vancouver Island in the ray trace model, which is required by a 1 second travel time offset across Georgia Strait (Ellis et al. 1983), corresponds fairly closely to the position in Riddihough's model where the subducting lithosphere dramaticly increases its dip. The presence of the Moho in the ray trace model at about 40 km depth emphasizes the existence of a seismic discontinuity where no comparable density discontinuity is present in the gravity model.

The reflection lines also indicated the 15.5 km reflector of McMechan and Spence. The reflector at depth 24km, for which no corresponding boundary exists in the refraction models, indicates the upper boundary of the subducting oceanic lithosphere at this depth. The possible reflector near 36 km correspounds reasonably with the base of the subducting oceanic lithosphere. Further, the dip of 5

degrees corresponds closely to the one of about 6 degree proposed by the Riddihough model and the refraction models.

The preliminary analysis of reflection seismic profiles which were conducted in the south Vancouver Island as part of the Lithoprobe project shows a strong reflection, which is about 20 km beneath the west coast of the Island and 31 km beneath the east coast, and is considered to be the top of the underthrusting oceanic crust (Yorath et al, 1984; Green et al, 1985a, 1985b). Figure 9 shows the preliminary interpretation of the Lithoprobe VISP1. Towards northern end of VISP1 there is some evidence for an increase in dip of the reflector, beyond here continuity is lost. The apparent absence of the deepest reflections beneath the northernmost region of VISP1 yields two possible explanations. One is probably related in some way to geological and topographic complexities because the profile tranverses the nose of NW-SE trending anticlinal ridge; another is that the dip of the subducting plate increases suddenly to a value in excess of 45°. The relatively conventional data processing would have filtered out any reflections from that zone. Above this reflector a region with high density/high velocity has led to the suggestion that it represents an underplated slab of oceanic lithosphere, perhaps a remnant of an earlier phase of subduction. This underplated slab corresponds to the large block of anomalous material in the gravity model (Green et al, 1985a, 1985b). Figure 10 shows the velocity model and tectonic cross-section across the continental

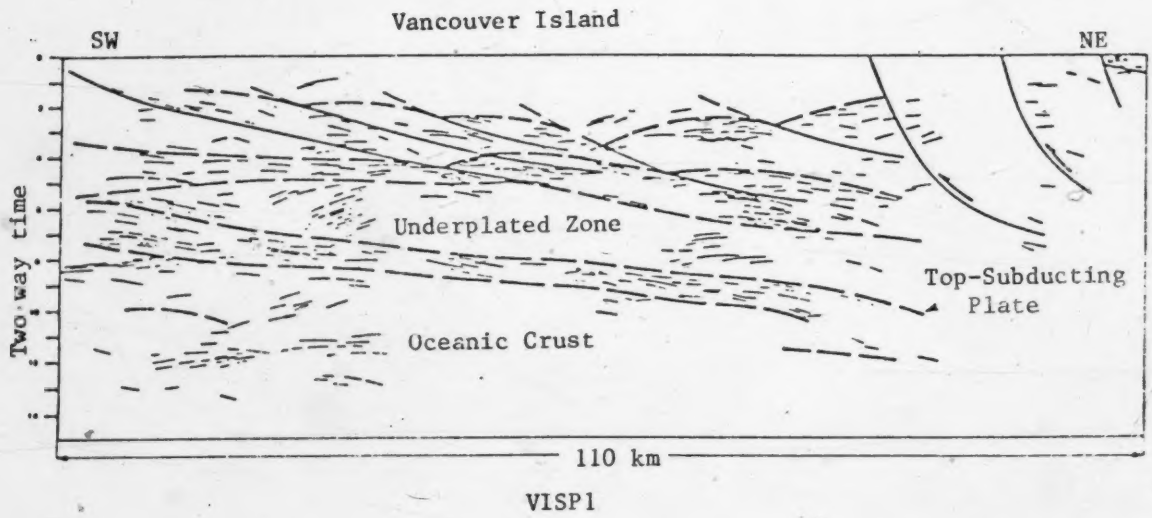

Figure 9.... shows the preliminary interpretation of Lithoprobe VISP1. Modified from Yorath at el 1985.

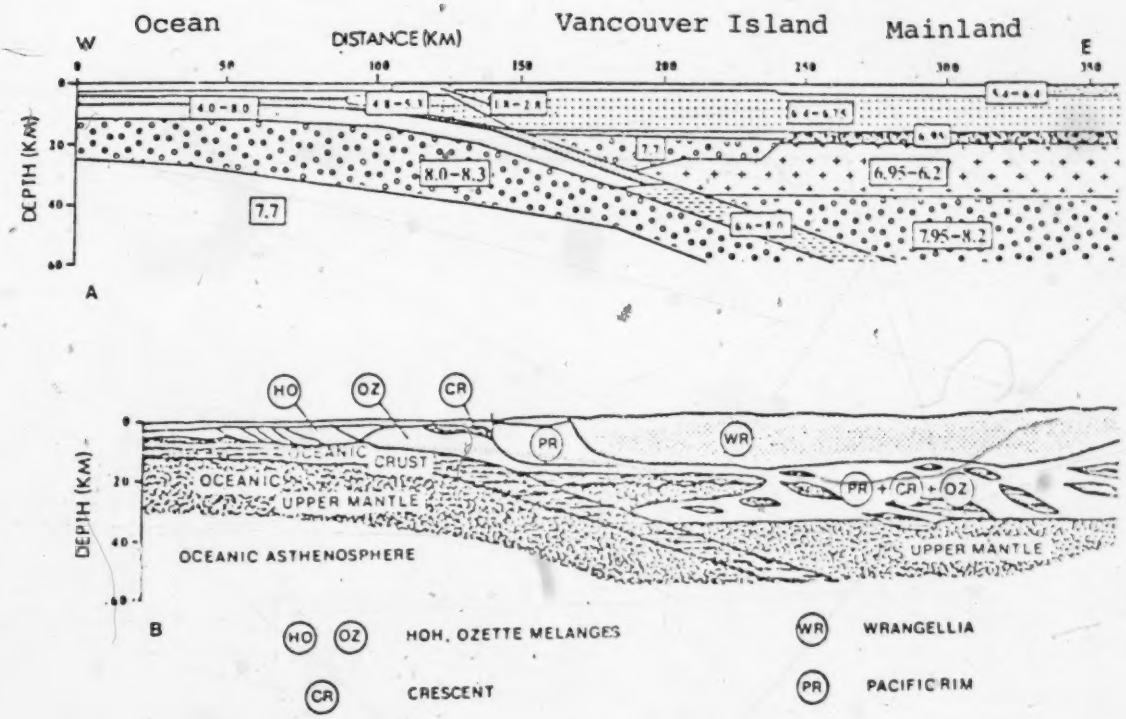

Figure 10.... shows the velocity model and tectonic cross-section across the continental margin. Modified from Yorath et al. 1985.

margin (Yorath et al, 1985).

1.4 Tectonic Stress related Earthquake Phenomena

Plate tectonics is understood to be new oceanic floor forming by solidification of molten rock in an opening crack, the oceanic ridge, and being consumed by subduction, forming an oceanic trench and generating earthquakes. In the area where two plates collide with each other stress concentrations appear, and the seismicity observed in the region must be representative of the state of stress that prevails in it.

Crustal stress can be investigated by means of field studies of recent movement on faults, or through overcoring strain relief techniques and hydraulic fracture experiments. The problems of these direct measurements of stress are that measurements are local and shallow, and many measurements are needed in a region in order to determine the average behaviour which will give the regional character of the state of the stress. The technique of modelling is another way to approach the problem of estimating stresses in the lithosphere, if we accept the major geophysical observables of heat flow, seismic data, gravity and plate velocity as constraints. The difficulty in modelling is that most of the parameters used, especially those for deep part of the earth, have to be estimated. The only constraint on the result is that the observed seismicity occurs in the unstable area, which is a region with high shear stress and

low strength of the material. Therefore we can not expect more than a general view of the state of the stress from the modelling technique.

The study of the seismicity catalogs for different parts of the earth shows that large earthquakes repeat at more or less fixed intervals in a region. The assumption that the rate of accumulation of stress is constant has led to the development of several different types of recurrence patterns (Shimazaki and Nakata, 1980). One assumes the upper level of stress at which the earthquake initiates is constant. This model implies that the stress is accumulated until it reaches this level, then an earthquake takes place and the stress level drops to a smaller level and the cycle starts again. Another model suggests the lower stress after the occurrence of any seismic event is constant. These patterns enable us to predict either the time of an event based on the size of the previous one or the size based on the time of the previous one. There will be no regularity if both upper and low level of stress are time dependent.

Another pattern for large earthquake occurrences in time and space is that large events appear to affect the seismic behaviour of zones which are very far away, and some large events seem to be preceded by anomalous seismic behaviours (Keilis-Borok et al. 1972, 1980). Lamoreaux (1982) summarised these patterns as a combination of quiescence and activation, the former refers to a spatial-temporal reduction (gap) and the latter to an

increase of seismic activity in comparison to the normal activity. Many of these patterns have been identified with the seismicity rate, the magnitude and the seismic energy released. Several qualitative theories have been proposed to explain these patterns physically; these include inhomogeneities in physical properties of the materials along a fault zone and the processes of crack population growth, independent of the material in which these cracks are formed. There is no satisfactory physical explanation for the occurrence of these patterns.

1.5 Earthquake Activity in the Vancouver Island Region

Milne (1978) pointed out that most of the seismicity on the western Canada margin has been concentrated along the three major plate boundaries, the Queen Charlotte -Fairweather fault system (Pacific-America plate), the offshore ridge-fracture zone system (Pacific-Juan de Fuca plates), and Vancouver Island-Puget Sound region (Juan de Fuca-American plates). The earthquake epicentres of the western Canadian margin are plotted in Figure 11. Unfortunately the focal depth data are not complete, only the earthquakes after 1978 have reasonable records for focal depth. The earthquakes in the rectangle, which is the area studied in this thesis, are projected into a cross section. The distribution of those foci for which we have reasonable depth are shown in Figure 12. The earthquakes with magnitude smaller than 4 are denoted by a small square; and those with

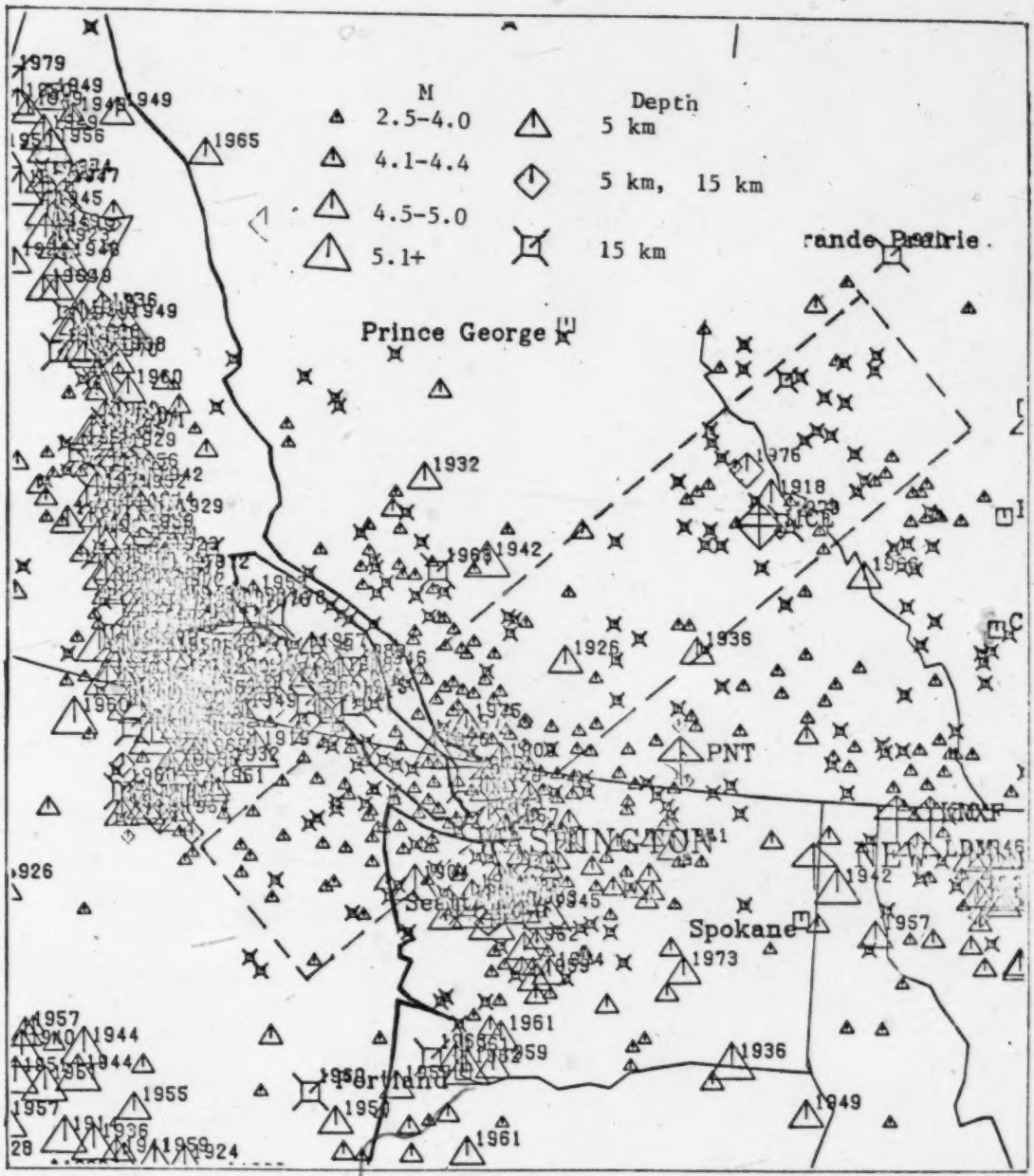

Figure 11.... shows the earthquake epicentres of the western Canadian margin. The area in the rectangle is studied in this thesis.

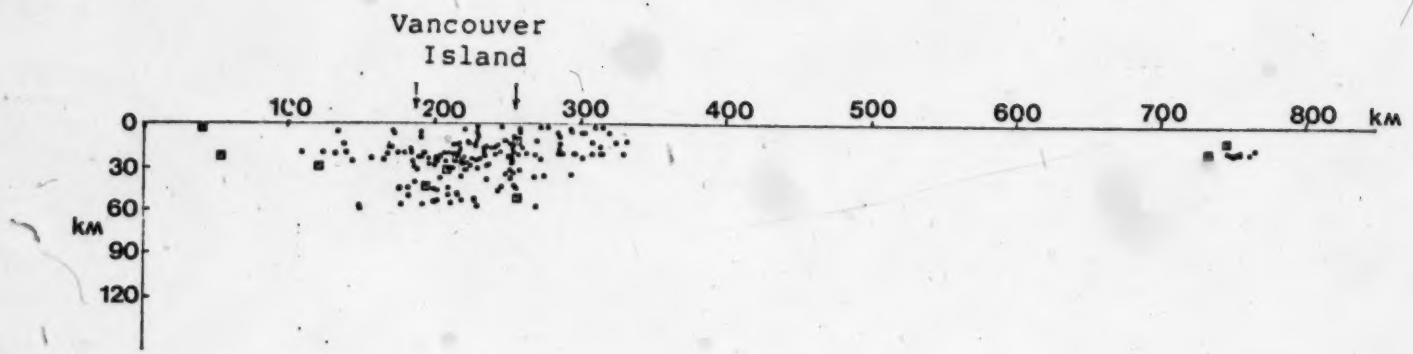

Figure 12.... shows the distribution of the foci of the earthquakes within the rectangle in Figure 11.

magnitude larger than 4 are denoted by a big square. Those earthquakes associated with the Queen Charlotte fault, the ocean ridge system and Puget Sound region may be in different stress environments from those in Vancouver Island. The distribution of the foci shows that the Benioff zone does not exist in that region and most of the earthquakes concentrate in the region beneath Vancouver Island, where the oceanic plate interacts with the continental plate. A fault mechanism solution study (Roger 1979) shows that the predominant type of fault mechanism for the large events is strike-slip, either dextral slip on a northwest trend or sinistral slip on a northeast trend.

II. The Model of Vancouver Island Subducting Lithosphere

The state of stress in a subduction zone depends on several features, such as the properties of the materials of the lithosphere and the geometrical structure of the subducting plate and its surrounding zone. The oceanic lithosphere increases its rigidity and its thickness as it moves away from the ridge at which it is generated (Forsyth, 1979). It is also generally assumed that the upper part of the plate behaves elastically and it starts to act in a viscoelastic way when its temperature increases (Solomon, 1980). Therefore the lithosphere can be thought an elastic layer over a high viscosity layer. Nevertheless this can only be the representative of the upper a few tens of kilometers of the earth's crust, where the temperature of the lithospheric material is below 300°C. This temperature is accepted as the limit for elastic behaviour. Below this temperature the thermally induced stress is small and the tectonics is describable by elastic stress (Turcotte, 1974). Above this temperature the thermal dependence of the stresses plays an increasingly important role in the overall state of stress as the temperature goes higher.

From a quasi-static point of view, Young's modulus E should become smaller as depth increases because the material is becoming more ductile as temperature increases. Kirby (1977) suggested an exponential dependence of Young's modulus E with temperature, which is taken to be

$$E=E_{min}+E_0e^{-x}$$

where E_{min} is the lower limit of Young's modulus, E_0 equals E at the surface of the earth minus E_{min}, $x=T^2/C$, T is temperature and C=600 a consistant determined by experience.

Wiens (1983) shows that the depth of seismicity is temperature controlled and that the limiting isotherm is approximately 700°C-800°C. The limiting temperature for seismicity in shallow seismic slabs is about 600°C (Molnar et al. 1979). Lithosphere thickness is inferred from a variety of techniques which yield different results. The elastic thickness is derived from the response of the lithosphere to long-term loads which agrees with the seismically active thickness of the lithosphere (Watts et al. 1980), whereas the seismic thickness is taken from its response to its short-term loads, which is about twice the elastic thickness (Leeds et al. 1974). Thus earthquakes occur primarily in areas of lithosphere which can sustain long-term loads as identified by studies of flexure. The elastic thickness is dependent on the flexural rigidity D, which is given by (Watts et al. 1980)

$$D=Eh^3/12(1-\nu^2)$$

where h is elastic thickness, ν is Poisson's ratio, and E is Young's modulus. Most of these elastic thicknesses were computed by assuming a 'seismic' Young's modulus E, this

estimate gives the result that the elastic thickness is slightly less (about 10 percent) than the seismically active thickness (Wiens, 1983; Watts et al,1980). Under long term loads, the time dependent effects of the material will be significant. Besides the elastic deformation the materials will show a creep effect. It seems that the material will become "soft". Therefore, Young's modulus should be smaller than the "seismic" estimate for the response of the lithosphere to long-term loads in the elastic approximation. To match the elastic thickness with the seismically active thickness of the lithosphere, Young's modulus E would decrease about 20 percent.

The relation between the adiabatic (dynamic) and isothermal (static) parameters can be found directly from:

$$E_d = E/(1-ET\alpha^2/9C_0)$$

$$\nu_d = (\nu+ET\alpha^2/9C_0)/(1-ET\alpha^2/9C_0)$$

where C_0 is the specific heat per unit volume at constant pressure. E_d and ν_d are the dynamic Young's modulus and Poisson's ratio (Landau and Lifshitz, 1970). Nevertheless, this kind of difference between dynamic and static parameters only makes their values vary by a small percentage. At 1500°K the difference between E_d and E is less than 5 percent.

The temperature distribution in a sinking slab beneath islands arcs was calculated by McKenzie (1969). The

temperature inside the subducting slab with a constant velocity are governed by (McKenzie 1969)

$$\frac{\partial^2 T'}{\partial x'^2} = \frac{\partial^2 T'}{\partial z'^2} + \frac{1}{R^2}\cdot\frac{\partial^2 T'}{\partial x'^2}$$

where T', x', z' are dimensionless quantities, R is the Thermal Reynolds number

$$R = \frac{\rho C_o v l}{\kappa}$$

The solution of this equation is of the form

$$T' = 1 + 2\Sigma \frac{(-1)^n}{n\pi} \exp\left(-\frac{n^2\pi^2 x'}{R}\right)\sin(n\pi z')$$

Figure 13 shows the isotherms within the sinking slab with the parameters used as

$v = 10$ cm/yr, $\rho = 3$ g/cm^3

$\kappa = 10^{-2}$ cal/cm degC sec, $l = 50$ km

$C_o = 0.25$ cal/gmdegC

The result shows that $0.6T_o$ isotherm will not vanish untill it reaches a depth down to 300 km. Therefore it is expected that the cold slab remains cooler than surrounding medium

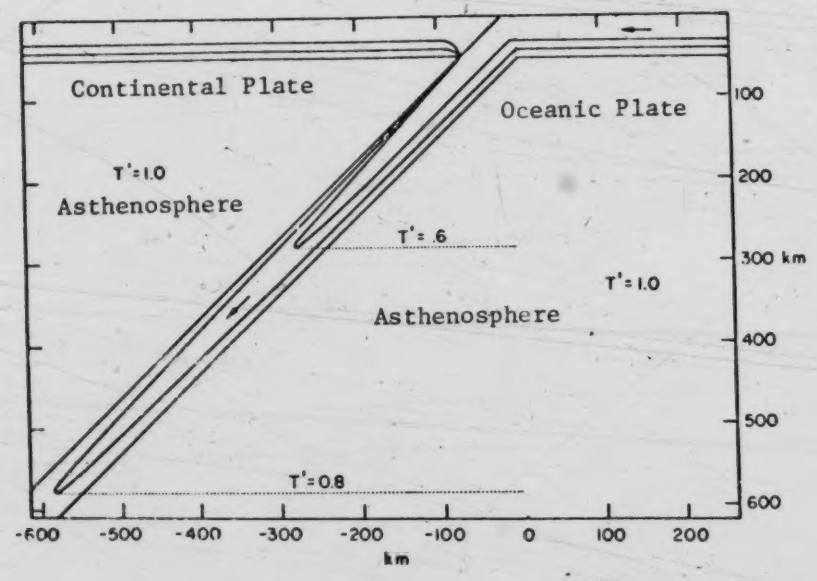

Figure 13.... shows the distribution of dimensionless temperature T' in a subducting plate. Modified from McKenzie 1969.

down to a certain depth beyond which the slab will become hot and soft.

Lewis (1985) gives a thermal profile for the Vancouver Island subduction zone. His results show that the temperature of the upper 20 km of lithosphere is less than 300°C. With reference to the McKenzie calculation (1969), the 300°C isotherm will reach a depth of 50 km in the model with a thickness l=30 km and velocity v=4 cm/yr, which is the case in Vancouver Island. Therefore the elastic model will give a reasonable approximation for the upper 20 km of the lithosphere and down to about 50 km for the sinking slab.

2.1 The Finite Element Model and Boundary Conditions

The finite element technique is one of the most useful methods in stress calculation. The results from recent geophysical studies on Vancouver Island have given us valuable data on the plate tectonic regime and subduction structure of the region. These yield comprehensive constraints on our finte element models.

The analysis of the stress state at the Vancouver Island subduction zone is reduced to a two dimensional problem here. The model is taken along a line crossing Vancouver Island and perpendicular to the continental coast line. It represents a cross-section within the rectangle in Figure 11. Since the Juan de Fuca plate has moved about N35°E relative to American plate for last million years, I

assumed the driving force on the Juan de Fuca plate takes the direction in which it moves related to American plate. This force therefore can be modeled by adding a load in our two dimensional model.

The geometrical structure and the velocity structure are based on the model shown in Figure 10 (Yorath et al., 1984). It is constrained by the VISP seismic structure and recent results from Lithoprobe Project (Introduction 1.3). In the model the subducting plate dips at 10° from base of the continental slope, then the dip increases to 18° and it continues plunging at this angle down to 200 km depth. The shallow dip part of the model in the sea is constrained by the seismic refraction profile (Ellis et al. 1983). Beneath Vancouver Island the dip of the sinking slab can be constrained by the data from onshore and offshore seismic refraction and reflection surveys. The shallow part of the model is also consistent with the gravity data. The deep parts of the model are weakly constrained because of the absence of deep reflections.

According to recent interpretations of the seismic survey line VISP1 (Introduction 1.3), the subducting plate dips at 9° to 16°, probably increasing to a value in excess of 30° at end of VISP1. There is a possibility that the subducting plate begins to plunge steeply into the mantle at this point.

The degree of dip of the subducting slab is directly related to the degree of mechanical coupling between the two

lithospheric slabs. It has a close relationship to the rupture length of earthquakes (Kanamori, 1977; Uribe-Carvajal, 1984). Uribe-Carvajal (1984) calculated several models with different angle of subduction and concluded that the stability distribution depends on the angle of the subduction or the degree of the mechanical coupling between the plates.

The top layer over the oceanic plate, with the compressive velocity about 2 km/sec, can be neglected in the geodynamic study because it consists of the soft Quaternary sediments. The remaining layers are simplified as shown in Figure 15 . Theoretically, Poisson ratio ν changes within the range from 0 to 0.5. For most crustal rocks ν is around 0.25 and it is a common assumption in geophysical modelling to use values between 0.25 and 0.3 for Poisson's ratio (Uribe-Carvajal, 1984). In this model 0.25 is used for surface rocks, and 0.3 is used for the rocks in the lower layer of the plate.

The values for the density of the materials in the model are inferred from the gravity model constructed by Sweeney et al (1985) based on Lithoprobe seismic reflection and gravity measurements. With Poisson ratio ν and density ρ determined as above, the Young's modulus E can be calculated from the compressive velocity by the formula

$$E=\frac{\rho\alpha^2(1+\nu)(1-2\nu)}{(1-\nu)}$$

where α is the compressive velocity, ρ and ν are density and Poisson ratio respectively. This calculation gives the values for short term load response. I would take 20 percent from the E calculated with above formula in this static problem for the reasons discussed previously. All the parameters used for this model are listed in table 2.

Kanamori (1980) summarises the various forces that have been postulated as driving a plate motion. Among these are 1) gravitational pull of a dense subducted slab at an island arc, 2) gravitational sliding or pushing from ocean ridges, 3) viscous drag due to the convection currents in the asthenosphere. The forces that resist plate motions are 1) frictional force acting on the fault plane of thrust earthquakes at subduction zones and of strike slip earthquakes along transform faults, 2) viscous resistance due to the asthenosphere.

It is controversial whether the asthenosphere resists or drives the motion of the lithosphere. The forces from ridge push and gravitational pull are two major forces that drive the plate and are the same for all trenches and ridges regardless of spreading rate. Therefore, small plates should move faster than large plates under the constant passive drag force and vice versa under active drag force. The observation of global plate motion (Kanamori,1983; Le Pichon, 1968) shows no substantial relation between velocities and plates, which implies the viscous drag may or may not act as a passive force on the plates.

Table 2: Parameters of the model

Index of Materials	Compresive Velocity km/sec	Young's modulus $\times 10^{12}$ dyn/cm^2	Poisson ratio	density g/cm^3
1	7.0	0.954	0.25	2.92
2	8.2	1.335	0.3	3.34
3	7.7	1.039	0.3	2.295
4	6.75	0.887	0.25	2.92
5	6.4	0.711	0.3	2.92
6	7.7	1.163	0.3	3.30
7	8.0	1.249	0.3	3.285

The viscous drag stress per unit length (Richardson, 1978) is

$$\tau = \eta V/h$$

where V is the velocity of the plate, η and h the viscosity and the thickness of the asthenosphere. Uribe-Carvajal (1984) assumed, in his study of thermo-elastic behaviour of subducting lithosphere, that at the bottom of the asthenosphere no displacement is possible, and the drag force opposes the direction of plate motion and is a function of the thickness of asthenosphere (h).

The value of viscous stress τ can be estimated by means of a thermal convection model. Mantle convection has been considered as an important energy source for driving plate motion and causes other geophysical and geological phenomena. Such convection happens in the upper and low mantle and core, and through this convection most heat is transfered to the surface of the earth. Stacey (1977a) has simplified such thermal convection to a heat engine problem. The output of the mechanical work of the heat engine is used to overcome the viscous force in the mantle and frictional force between plates. In his model the engine is working between high temperature T_2 and low temperature T_1 (Figure 14). The circulation of the heat engine is composed of two adiabatic processes and two isobaric processes. The efficency and power of the heat engine are calculated. Table

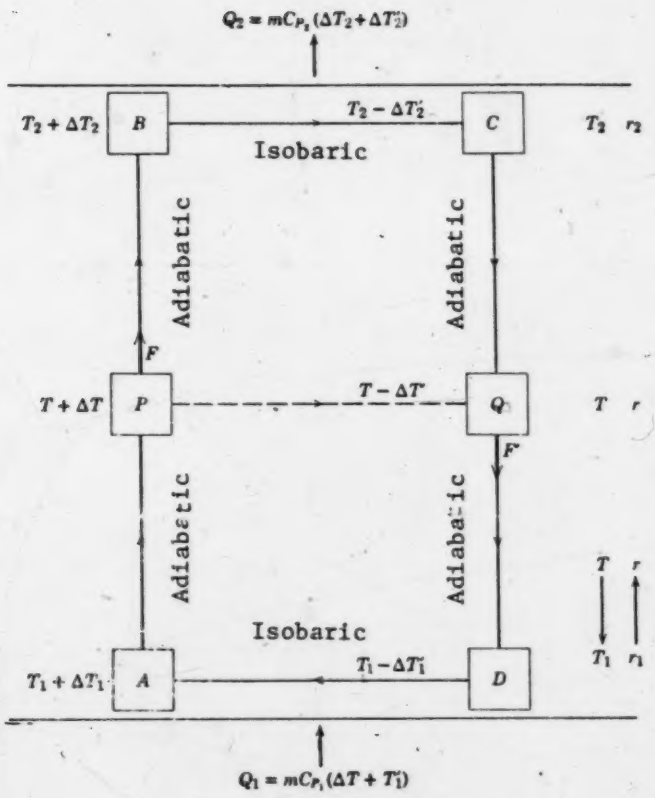

Figure 14.... shows Stacey's heat engine for mantle convection. The path A→B and C→D are adiabatic processes, path B→C and D→A isobaric processes. Modified from Stacey 1977.

Table 3: Thermodynamic Efficiency and Power of Core and Mantle Convection.

Zone	Assumed Heat	Efficiency	Power
Outer core (self-heat)	5×10^{12} W	5.5%	$0.27, \times 10^{12}$ W
Lower mantle			
Core heat	5×10^{12} W	21.1%	$1.0, \times 10^{12}$ W
Self heat	11×10^{12} W	10.6%	1.2×10^{12} W
Upper mantle			
Core heat	5×10^{12} W	10.6%	0.5×10^{12} W
Lower mantle heat	11×10^{12} W	10.6%	1.2×10^{12} W
Self-heat	6×10^{12} W	6.0,%	0.36×10^{12} W
Crust	9.5×10^{12} W	—	—

3 lists these data for different part of the earth (Stacey 1977).

The estimate of the drag force can be made with the following model (Stacey 1977b). Considering a plate with area A and thickness d, deformation of the plate will occur if a shear stress τ is applied to the surface of the plate. If the top of the plate moves with velocity v over the bottom, the energy consumed should equal to the work done by the force τA:

$$dE/dt=\tau Av$$

According to the data in table 2, we can assume the power of convection of the upper mantle as 1.0×10^{12} watts. For the upper mantle and crust, the power of convection per unit area is 2×10^{-3} w/m^3. If the oceanic plate moves with velocity of 4 cm/yr ($v=1,3\times10^{-9}$ m/sec), the stress corresponding to the consumed energy can be calculated with above formula, it gives $\tau=15\times10^5$ Pa (or 15 bar). Although this method gives a very rough estimate, it explores the order of magnitude of the viscous drag force on the plate.

The mean pressure exerted on the lithosphere by the ridge can be estimated by (McKenzie 1969)

$$\Delta p=\frac{1}{2}g(\rho_0-\rho_s)e$$

where e is the elevation of the ridge above the deep sea

floor and ρ_0 and ρ_w are densities of the lithosphere and sea water respectively. Substitution of

$$e=2 \text{ km}, \quad \rho_0-\rho_w=2 \text{ g/cm}^3$$

gives

$$\Delta p=0.2 \text{ kbar}$$

The application of realistic boundary conditions is often a difficult problem. Here in order to simulate the boundary condition at infinity on the left side of the model (see Figure 15), increased loads with depth are applied atthe left side to balance the horizontal components of the stress due to gravity. The right side and bottom of the model are fixed. As calculated above the force on the oceanic plate due to ridge push is about 0.2 kbar. It is a difficult problem to impose this force on this finite element model, because the boundary between the oceanic plate and the asthenosphere below it is set as a solid boundary, that is the relative movement is not allowed at the boundary. If we add a force at the left side of the upper part of the model, this force will not affect the area which is far away from the left side of the model. This occurs because the force will be balanced by the shear stress due to shear strain generated in the area close to the place where we add the force. Therefore the effects due

to the ridge push and the viscous force on the base of oceanic crust can not be simply modelled by adding the force on the oceanic plate to the left side of our elastic model.

To overcome this difficulty in our elastic model we consider that the net force exerted on a part of the plate from the ridge push should balance the viscous drag on the base of that part of the plate. Therefore we can assume a body force on the oceanic plate which equals the viscous drag due to asthenosphere. This force will balance the viscous drag and the friction at plate boundaries and keep the plate moving steadily. Therefore, this force will give the effect of interaction due to viscous and frictional force at the plate boundaries on either continental plate or oceanic subducting plate itself. Neverthless, the effects on the stress state within the oceanic plate due to the ridge push can not be modeled in this way. The ridge push will cause about 200 bars additional stress with large principle component along the oceanic plate at the place close to the ridge, and it decreases gradually as the plate moves away from the ridge. This equivalent body force is determined by the viscous drag force which can be estimated as above.

At the convergent margin the force gets larger because the frictional force appears in addition to viscous force, and then it reduces to zero gradually as the slab plunges deeper into the upper mantle. In that case part of the viscous drag force is overcome by gravitational pull on the slab. The same kind of modelling is used in the case that

the mantle drag acts as an active force on the oceanic plate.

The model for this problem. is shown in Figure 15. It is a useful modelling technique that the initial model of the subduction zone is treated as a elastic model, then refined to show how the results change as the model becomes more complicated. This approach has proved useful in seismic stability studies (Uribe-Carvajal and Nyland, 1983 a b). In this thesis I discuss only elastic model. As mentioned above this model would only give a good approximation for upper 50 km. Below that depth the thermo-elastic properties of the material becomes more and more important. Neverthless the elastic model will enable us to get a basic understanding of the physical behaviour of the deep part of the subducted plate.

BLOWUP BACK REDRAW RDWO ADDNODES SUBNODES
ADDELEMS SUBELEMS WRITE STOP SCREEN DUMP DRWNEWP
MVNOD

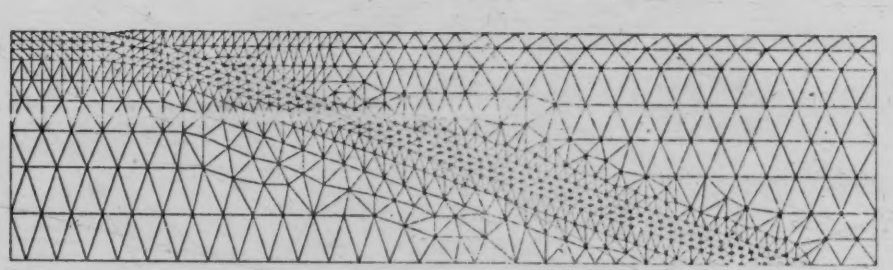

0 100 200 300 km

Figure 15.... shows the nodal distribution and the structure of the finite element model. The commands on top are used for modifying the model; see Appendix.

III. Analysis of Stress State and Instability

An earthquake can be thought of as a sudden failure of rocks, which is governed by the distribution of the stress within the lithosphere. Therefore analyzing the distribution of the stress in the subducting zone is important in study of seismic activity. In order to relate the stress distribution more closely to seismic risk the concept of instability will be introduced in this chapter. The risk probability function will be constructed from the theory for a Griffith crack (Jaeger and Cook 1979). The distribution of such probability will demontrate seismically dangerous locations. By relating seismicity to the instability distribution, we can discuss how the seismicity is affected by the tectonic stress, and in turn understand what kind of state of tectonic stress is possible.

Considering the effects of the driving mechanism on the seismicity of Vancouver Island, models with different driving mechanism are analysed in this chapter. The analysis allows the suggestion of a possible relationship that may exist between driving forces due to the oceanic ridge and asthenosphere and the seismicity at upper part of the subduction zone which is located beneath Vancouver Island.

3.1 The Concept of Stability

The failure process of the rocks is related not only to the concentration of stress within rocks, but also to the strength of the rocks. It is useful to introduce the concept

of stability in analyzing rock failure risk. This was first used in seismic risk study by Uribe-Carvajal and Nyland (1985).

For a two dimensional problem it is convenient to use the Mohr circle representation which gives the relation between shear stress and normal stress. The Mohr-Coulomb failure criterion is an appropriate failure criterion used in rock mechanics. The physical significance of using a Mohr-Coulomb failure envelop is that the rock is taken to have a linear relationship between the critical shear stress τ and critical stress difference, $\sigma_1-\sigma_2$, that is required to reach failure. The Mohr-Coulomb criterion is given by

$$\tau=S_0+\sigma_n\tan\phi$$

where S_0 and ϕ are material constants. S_0, the shear strength under zero normal pressure, varies considerably from zero in fractured materials to about 50 bars for sedimentary rocks up to several hundred bars for igneous and intact materials. ϕ is the angle of shear resistance, which lies btween 20° to 45°. This criterion states that failure occures when the Mohr circle touches the Mohr-Coulomb envelope.

Uribe-Carvajal defined the stability at a certain point in the model as the minimum distance between the failure envelope and the Mohr circle of the stress state (Figure 16). The further the Mohr circle is from the failure

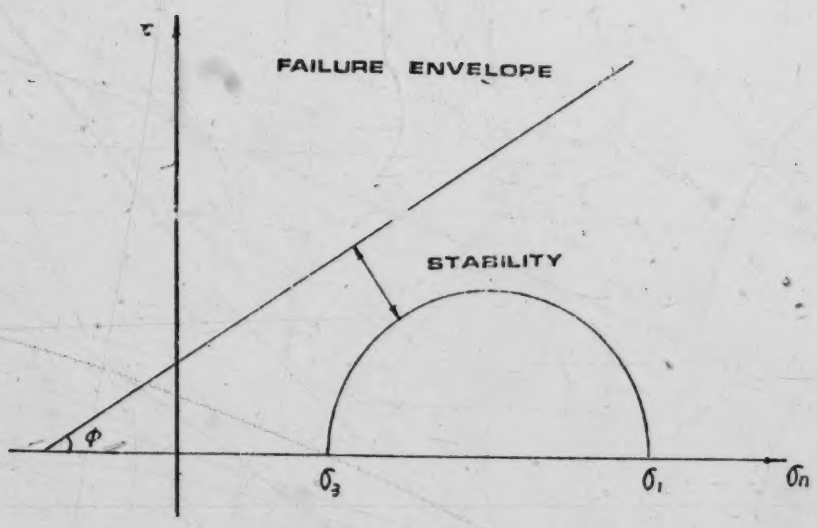

Figure 16.... shows the general definition of instability as the minimum distance from the surface of the Mohr circle to the failure criterion.

envelope the more stable the stress state is. The stability depends on the location and the model with which the stress distribution is calculated. It can be described as a functional

$$S(x)=S[M(x',p_i),x]$$

where p_i are the parameters of the model. After the model has been chosen, S(x) is only a function of location. If different models are used in the stability analysis, we can see how the stability is affected by the different models. The change of the stability with the models

$$\Delta S(x)=S[M_2,x]-S[M_1,x]$$

is defined as the residual stability. In the seismic risk study of the Valley of Mexico, Uribe-Carvajal used a residual instability as a measure of risk. This is derived by first estimating some form of average stresses in the area under investigation and then determining the stresses in an anomalous zone, subtracting from these stresses the normal stresses and calculating the distances of the Mohr circles for residual stresses from the failure envelope. In the following study, I will use effective shear stress and incorporate the concept of the Griffith crack to assess the measure of risk.

Griffith cracks are small flaws in rock, which I assume to be isotropically distributed in orientation. The failure of rocks takes place from these flaws. However, there seems no reason why it should not be applied to the behaviour of much larger cracks using a scale at which rock can be regarded as homogeneous, thereby providing an approach to the growth of fractures in rocks. We could assume the crust and mantle are homogeneous and contain a lot of cracks, and failure will happen when those cracks are in unstable equilibrium.

With an assumption of external stresses being held constant while the cracks extend, the condition for unstable equilibrium of a crack of length 2c in a material of thickness t is (Jaeger and Cook, 1979)

$$\frac{\partial}{\partial c}(W-4\alpha ct)=0$$

where W is the strain energy of the body, α is apparent surface energy density of the fracture. For a rectangular plate of length l, width b and thickness t, containing a flat elliptical crack of length 2c extending along the direction of the thickness, the strain energy W in the plate for conditions of plane strain is

$$W=W_0+\pi c^2 t(1-\nu^2)(\sigma_n^2+\tau^2)/E$$

where W_0 is the strain energy of the plate without the crack, E is the intrinsic Young's modulus, σ_n is the stress perpendicular to the crack, and τ is the shear stress parallel to the crack. In the case of a closed crack the effective stress, $(|\tau|-\sigma_n\tan\phi)$, is the only component of stress free to generate additional strain energy around the crack. Hence, the strain energy of the body can be obtained by substituting $(\sigma_n^2+\tau^2)$ for the effective stress. If the cracks are randomly distributed a spherical average may be taken over all directions, this yields a factor 1/3. The strain energy then wrtten as

$$W=W_0+\pi c^2 t(1-\nu^2)(|\tau|-\sigma_n\tan\phi)^2/3E$$

The criterion at which the crack will begin to grow, that is the failure will happen, for the case of a closed crack is, therefore, given by

$$(|\tau|-\sigma_n\tan\phi)^2\geq 2\alpha E/\pi c(1-\nu^2)$$

Or in another word, under the effective stress $|\tau|-\sigma_n\tan\phi$ the cracks which satisfy the condition

$$c\geq 2\alpha E/\pi(1-\nu^2)(|\tau|-\sigma_n\tan\phi)^2$$

will fail. Thus, the strength of rocks is closely linked to the size of cracks.

Physically, one can think of the failure criterion as being controlled by the distribution of cracks of various size in the body, therefore it is appropriate to use probability to describe the possibility of rock failure. Generally it is difficult to determine what kind of distribution the cracks in a body will follow. However, a variable will generally distribute normally if the value is influenced by a number of factors, and none of those factors have a dominant influence on it. Since we do not know what will be dominant effects for the crack distribution, I would think a normal distribution might be a reasonable form for the crack distribution in a body. Other distributions are also possible. For the sake of mathematical simplicity, I assume the cracks of various size in the body are distributed as

$$P_0(c)=2c/\sigma^2 \cdot \exp(-c^2/\sigma^2)$$

Figure 17 shows the values of $P_0(c)$ calculated for $\sigma=0.1$. This distribution has a similar form to a normal distribution, but $P_0(c)=0$ when $c=0$, hence the number of cracks with zero length is zero. This is more reasonable than normal distribution.

If the rock contains only one crack, the size of which is controlled by P_0, the probability that the crack in the rock will begin to grow by stress $|\tau|-\sigma_n\tan\phi$ is given by the probability that the crack will be longer than critical. The

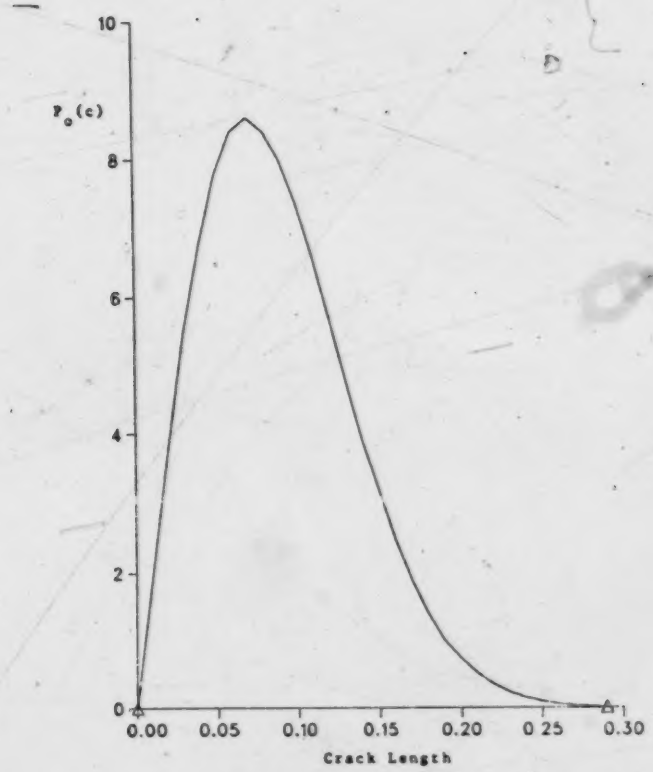

Figure 17.... shows the assumed distribution of cracks in a body. $P_0(c)$ is calculated for σ=0.1.

critical size is

$$c=2\alpha E/\pi(1-\nu^2)(|\tau|-\sigma_n\tan\phi)^2$$

therefore the probability, $1-P_0$, that the crack will not break is

$$1-P_0=1-\int 2c/\sigma^2\cdot\exp(-c^2/\sigma^2)dc=1-\exp(-c^2/\sigma^2)$$
$$=1-\exp(-\lambda^2/\sigma^2S^4)$$

where $\lambda=2\rho\alpha E/\pi(1-\nu^2)$, $S=|\tau|-\sigma_n\tan\phi$. However, a body usually has many cracks within it. The idea that one part of the body is more stable than another suggests that the probability of failure of the cracks within some volumes of the body may be smaller than others. If we assume the body contains n cracks per volume, we will think this part of the body fails if at least one of those cracks begin to grow. Therefore the probability, 1-P, that no cracks within the unit volume will begin to grow as a result of the stress $|\tau|-\sigma_n\tan\phi$ is the product of the probability that an individual crack will not begin to grow, that is

$$1-P=(1-P_0)^n=(1-\exp(-\lambda^2/\sigma^2S^4))^n$$

This gives

$$P=1-(1-\exp(-\lambda^2/\sigma^2S^4))^n$$

Figure 18 shows values of P calculated for $\lambda^2/\sigma^2=7\times10^3$, n=100.

Since the value of λ and σ are unknown, it is generally convenient to introduce a relative measurement which will indicate that some area is closer to failure than others. But close does not mean that at a location with high probability value an earthquake must occur. This relative stability only gives a comparative measure for all different parts of the model (Uribe-Carvajal, 1984). Let $S=(S-S_{min})/(S_{mx}-S_{min})$, where S_{mx} and S_{min} is largest and smallest of S respectively. In this case the variable S will range from 0 to 1.

The different values of λ, σ and n will not change the basic shape of the curve of the probability function. The only justification for the choice of these constants for this problem is to make the curve have a reasonable shape as S changes from 0 to 1. Here 0.116 and 1 are chosen for λ^2/σ^2 and n respectively. The frictional angle ϕ is chosen as 30° in the calculation in this thesis. In the following section, this probability function will be used in representing seismic risk in particular areas.

3.2 Instability Analysis for Vancouver Island Region

The state of stress of Vancouver Island was calculated with the two dimensional finite element model discussed in the previous chapter. The first model is calculated for the case that the area only suffers gravitational load. The

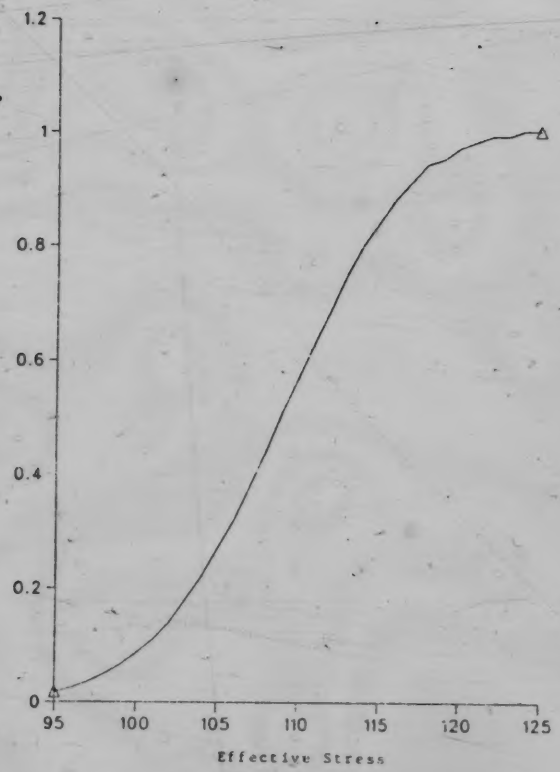

Figure 18.... shows the probability function of P, which is calculated for $\lambda^2/\sigma^2=7\times10^4$, n=100.

boundary conditions taken are as follows: the model is restricted to move in the vertical direction only on both left and right sides, on the bottom no displacement can take place. In order to explore the distribution of the anomalous stresses due to the structure of the model, the treatment of residual stress is useful. It is derived by subtracting an assumed gravitational stress field due to an infinite homogenous half space from the stress field calculated by the model (Uribe-Carvajal, 1984). Figure 19a shows the average stress distribution of the model, which is defined by $(\sigma_1+\sigma_2)/2$. Figure 19b shows the maximum shear stress distribution defined by $(\sigma_1-\sigma_2)/2$. The normal stress field due to an infinite homogenous half space was calculated by assuming the density ρ=3.0 g/cm^3 and Poisson's ratio ν=0.3. In Figure 19b we can see some contours along the lower part of the subducting plate.

Since the density of the upper mantle beneath the oceanic plate and that beneath the continental plate are quite different, it is difficult to find an appropriate density for the assumed infinite homogenous half space. Different densities were tried, but none gaves a better result.

The instability is calculated by means of effective stress. Figure 20 shows the distribution of the instability of the Vancouver Island region. The contours of equal instability show that the instability concentrates along the subducting slab. This implies that the sinking slab is more

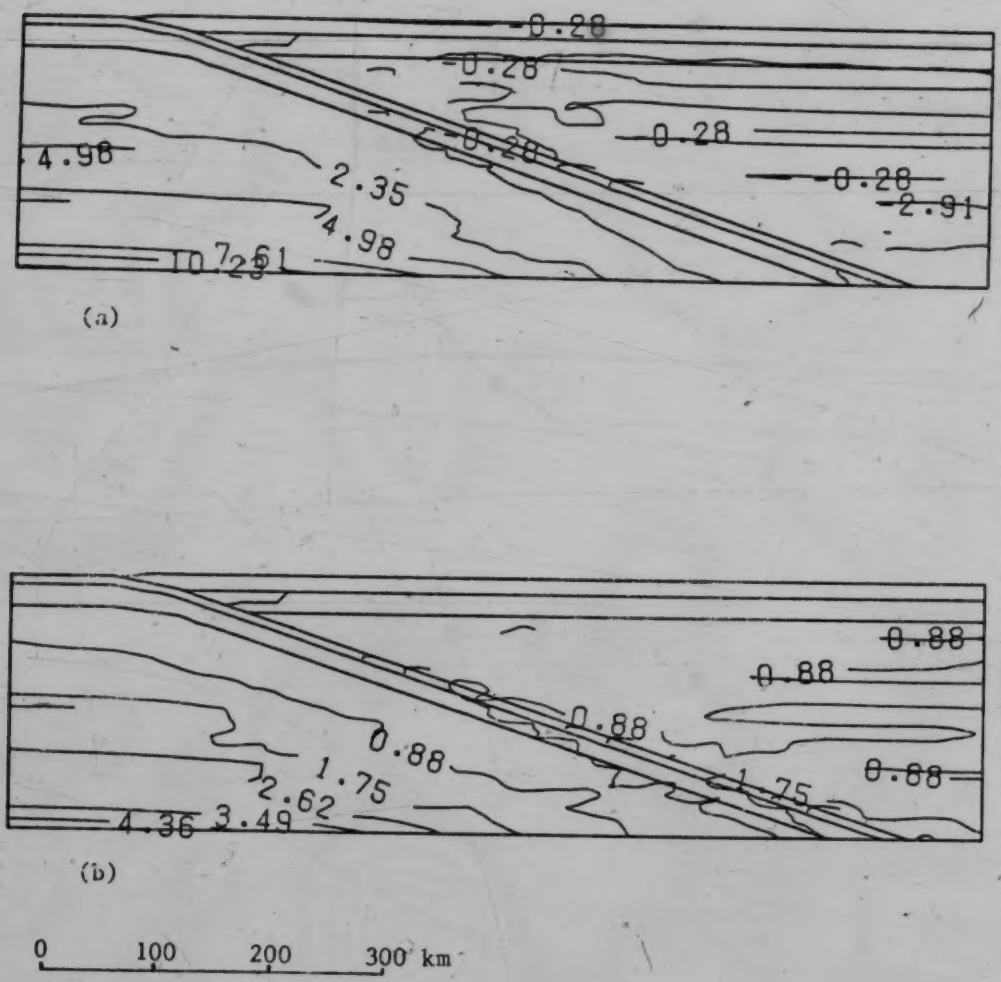

Figure 19.... (a) shows the average stress distribution and (b) the maximum shear stress distribution of the gravitational model.

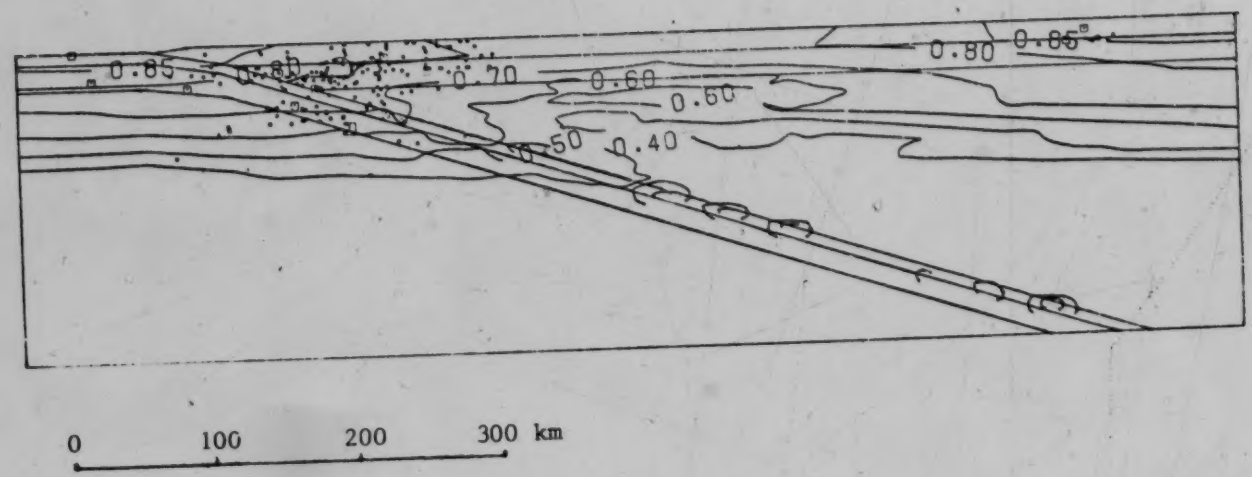

Figure 20.... shows the distribution of instability for the model only under the gravitational load.

unstable compared with its surrounding regions. Earthquakes will have a higher probability of happening within those regions. This phenomenon agrees with the concept of a Benioff zone and the general idea that the earthquakes occurring along the Benioff zone are probably due to gravitational stress. However the area beneath Vancouver Island, a region with anomalous structures, lacks such instability concentration.

To incorporate an external stress, it should be recalled that the driving tectonic stress introduced by the ridge push is about 200 bars, and a resistance force in order of 20 bars will be generated along the plate boundary. The second model is calculated for the case that there is an external force, from ridge push, exerted on the oceanic plate. In this model I assume a 20 bar viscous force acting on the bottom of the oceanic plate opposing the motion of the plate. At the convergent margin an additional 20 bars frictional force acts on the top of the oceanic plate. In the calculation these forces are changed to body forces acting on the oceanic plate for the reason discussed in chapter 2.

Figure 21 shows the instability distribution of the model and the distribution of the earthquakes that have occurred in that region. By comparing Figure 20 with Figure 21 it can be seen that the zone located beneath Vancouver Island became more unstable. The unstable zone which is enclosed by the contours can also be recognized by the fact

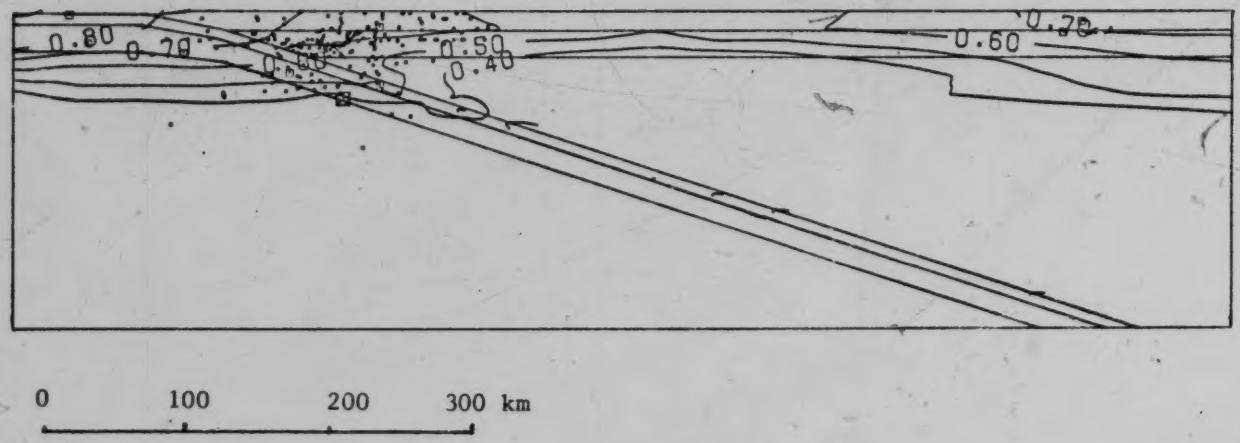

Figure 21.... shows the distribution of instability for the model with ridge push force exerted on oceanic plate.

that the earthquake foci concentrate in that region. The observed seismicity occuring in the area is one of the constraints on the model. The coincidence of the distribution of the instability contours and observed earthquake foci suggests that the force from ridge push has a direct relation to the seismic activity in the upper part of the subducting zone at Vancouver Island.

The force from mantle convection rather than resisting its motion can be considered a possible driving force for the motion of the oceanic plate. For this reason a model with a viscous force acting on the bottom of the oceanic plate in the direction of its motion was studied. In this model I added some force on the nodes beneath the oceanic plate in the model by assuming there are about 10 bars viscous force on the base of the oceanic plate.

Figure 22 shows the distribution of the instability for this model. Again in this model the contours are concentrated on the top of the subducting plate, the contours of value 0.4, 0.5 and 0.6 are all concentrated in the region located beneath Vancouver Island, and they do not show up at the right side of the model or in the deep part of the subducting plate. This result implies that under the applied force from gravitational ridge pushing and mantle convection the region located beneath Vancouver Island is more unstable than the rest of the model.

Comparing the instability analysis in models 1, 2 and 3, one of things we should notice is that the unstable zone

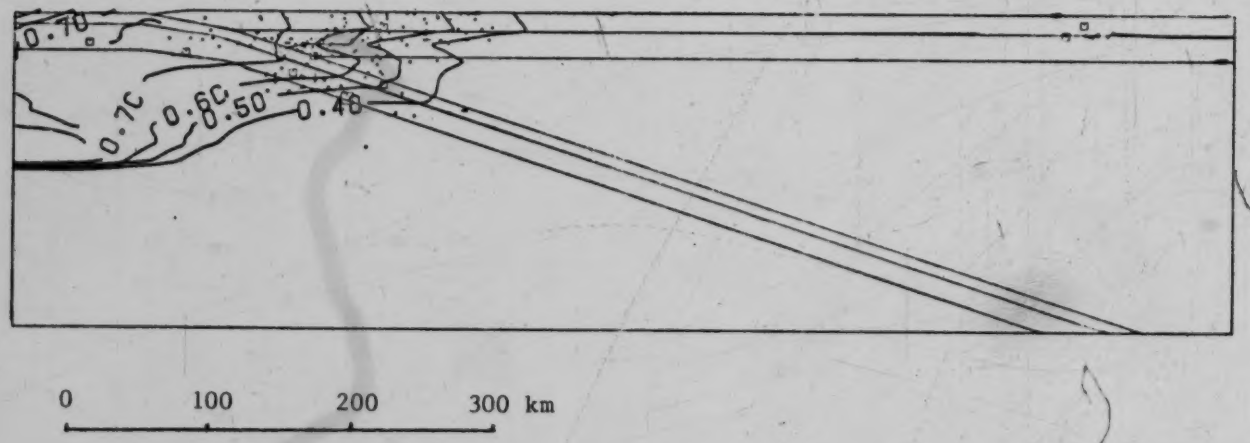

Figure 22.... shows the distribution of instability for the model with an active viscous drag on the bottom of oceanic plate by the asthenosphere.

at top of the subducting plate is probably caused by stress due to ridge push and mantle convection. The gravitational pull of the dense subducted slab seems not to affect that region very much. If this is true, the state of tectonic stress in that region is caused by the interaction between the oceanic plate and the continental plate under the forces due to ridge push and mantle convection and should be predominantly horizontal. This can be checked by the focal mechanism or fault-plane solutions of the large events in the study area.

Rogers (1979) studied the focal mechanism of normal depth earthquakes in the Vancouver Island region. He concluded that the predominant type of faulting is strike-slip, either dextral striking northwest or sinistral striking northeast, therefore the dominant compressive tectonic stress is acting with a north-south orientation. He suggested that the earthquakes could be responding to regional crustal compression caused by the Explorer-America and/or Juan de Fuca-America plate interactions. His result agrees with what we suggest from the modelling study. Although his suggested north-south compressive force can not be modelled in this two dimensional model, which is on an about northeast-southwest orientation, we can still compare the results studied by these two different methods.

It is accepted by most geophysicists and geologists that the Explorer and Juan de Fuca plates subduct beneath Vancouver Island, but the lack of a Benioff zone is still

controversial. As discussed above the concentration of the instability along the sinking slab could be responding to the stresses caused by the gravitational pull of the cold dense slab. The lack of a Benioff zone in the Vancouver Island region would suggest that no such gravitational pull acts on the deep part of the subducting plate. This suggests such a cold dense subducted slab does not exist in the deep part of the subduction zone. The heat flow study of the southwest British Columbia suggests that one of the possible reasons for high heat flow farther inland is the upwelling of magma and convective transport of heat from a sinking slab. Melting may commence when the slab reaches a depth of about 100 km. The area below critical temperature for earthquakes is above 70 km in a sinking slab (Keen and Hyndman, 1979). Since the sinking slab starts to melt at such a shallow depth, it will not generate a pulling force on the top plate.

We know generally there are three kind of forces which provide a driving mechanism for plate motion. Two of them, gravitational pull of a dense sinking slab and gravitational pushing from an oceanic ridge, are the same for different trenches. Whether the drag force between the oceanic plate and asthenosphere is passive or active depends on different regions. Previous discussions would lead to the suggestion that viscous drag force from the asthenosphere is one of the driving forces on the Juan de Fuca plate as it subducts beneath Vancouver Island. This force, as well as the

gravitational pushing from the oceanic ridge, could be directly related to the seismicity in the Vancouver Island region.

IV. Conclusions

This study has shown that from a knowledge of the geological structure and some geophysical data of the Vancouver Island region, a reasonable finite element model of the plate interactions can be built. The model used for the stability determination of the Vancouver Island region is restricted to elastic material and does not take into account the effect of temperature distribution. Nevertheless it can tell us something about the relation between distribution of seismicity and geodynamic processes of that region.

Instead of directly studying the distribution of stresses, the instability distribution, which is described by the probability of rock failure, was studied. One thing I have to emphasise here is that probability values are relative within a model calculation, therefore the actual value is just an indicator of where failure is more likely to occur for a set of given conditions. It is more reasonable to focus this kind analysis on the study of the distribution of high and low value areas rather than on the values themselves.

Analysis of the instability distribution shows that such a measure is very useful in studying the risk of seismic events. Although the distribution of the stress is also related to rock failure at certain points of the model, it could not give a clear picture of the unstable zone because of the dominance of the stress due to gravity. It is

difficult to determine the stress field due to a homogeneous infinite half space, from which we can distinguish the anomalous stress due to the structure or plate driving mechanism of the model. For this kind of study the effective stress is more capable in describing instability. It gives a better picture of instability distribution.

We can link the instability with the state of stress by different theories. In this study I use the concept of effective stress incorporated with a Mohr-Coulomb failure envelope, which means a linear relationship between critical shear stress and the difference between maximum and minimum principal stresses. The instability function is constructed by assuming a certain kind of crack distribution within the body. This enables us to have a basic physical understanding of the relations among the stress state, the crack distribution and the strength the material.

We know that most of earthquakes occur on a preexisting fault where the strength is lower, and some mechanical weak region probably corresponds to a high density of cracks. Since those elements can not be easily determined, I used the same strength for different materials distributed through whole model, therefore the distribution of the instability only gives a view of how a seismic dangerous region is affected by the tectonic stress. A particular local event can probably be caused by the weakness of the local material, but the regional seismicity should agree with the high instability region controled by tectonic

stress. I also neglect the effects of the interaction among those cracks, which may have an important effect on the crack propagation.

The study of how the distribution of the instability is affected by gravitational pull of a dense sinking slab or gravitational pushing from an oceanic ridge was made for the Vancouver Island region. The results of the analysis suggest that instability at the upper part of subducting zone is strongly linked to the driving forces from ridge push and mantle drag, however the force from gravitational pull of the dense slab has little effect on the upper part of the subducting plate. The instability concentrates in the region located beneath Vancouver Island when the interaction between the Juan de Fuca and continental plates is enhanced by introducing a frictional force between two plates. The observed seismic active area coincide with the instability concentrated area in the model. I therefore believe that the driving mechanism of the Vancouver Island subduction zone is provided by the gravitational pushing from the ridge and viscous drag due to the convection in the asthenosphere. The gravitational pull of the dense sinking slab does not exist, or makes a negligable contribution to the process.

These simple models do not address the more complex questions such as the mechanism of the mantle convection, and how the motion of the oceanic plate may be generated; they only provide an insight into some important aspects of the seismicity, the effects of interaction between plates

and of gravitational stress. We may have neglected some other factors which have major influence on the seismicity of the study region.

I would repeat here that the elastic model, which does not consider temperature effects, used for this study can only give a good approximation for the upper few kilometers. Since the heat flow of the study area is very high, suggesting the oceanic plate is melting at a shallow depth, it is important to take into account temperature effects on the model. Some geophysicists argue that fluid probably exists in a subducting plate. The existence of the fluid may strongly affect the distribution of the instability in its surrounding region. It would be an interesting problem to introduce a fluid into the finite element model.

A generally accepted idea about plate tectonics is that the elastic oceanic plate lies over a viscous asthenosphere. The plate subducts with steady speed into the upper mantle at the convergent margin, and begins to melt when it reaches high temperature in the deep part of the mantle. The effects of the oceanic plate over the viscous asthenosphere and of the melting part of the sinking slab on the motion of the sinking plate should be modelled in order to get a good approximation for the subduction region. This requires us to consider the time dependent effect of the viscosity of the asthenosphere and the temperature effect on the deep part of the model. To introduce these properties into a finite element model is not straightforward. A better result

probably can be achieved when the model is improved.

References

Barr, S. M. (1974). Structure and tectonics of the continental slope of southern Vancouver Island. *Canadian Journal of Earth Sciences* 11; 1187-1199.

Carson, B.; Yuan, J.; Myers, P. B.; and Barnard, W. D. (1974). Initial deep-sea sediment deformation at the base of the Washington continental slope: a response to subduction. *Geology*, 2; 561-564.

Ellis, R. M.; Spence, G. D.; Clowes, D. A.; Waldron, D. A.; Jones, I. F.; Green, A. G.; Forsyth, D. A.; Mair, J. A.; Berry, M. J.; Mereu, R. F.; Kanasewich, E. D.; Cumming, G. L.; Hajnal, Z.; Hyndman, R. D.; McMechan, G. A.; and Loncarevic, B. D. (1983). The Vancouver Island Seismic Project: a co-crust onshore-offshore study of convergent margin. *Canadian Journal of Earth Sciences* 20; 719-741.

Forsyth, D. W. (1979). Lithospheric Flexure. *Rev. of Geophys. and Space Phys.* 17; 1109–1114.
McKenzie, D. P. (1969). Plate Tectonics. in *The nature of solid earth*, Robertson E. C., Mcgrall Hill; 125–133.

Green, A. G.; Clowes, R. M.; Yorath, C. J.; Spencer, C.; Kanasewich, E. R.; Brandon, M. T.; and Brown, A. S. (1985a). Reflection mapping underplated oceanic lithosphere and the subducting Juan de Fuca plate. submitted to *Nature*.

Green, A. G.; Berry, C. P.; Spencer, C. P.; Kanasewich, E. R.; Chiu, S.; Clowes, R. M.; Yorath, C. J.; Stewart, D. B.; Unger, J. D.; and Poole, W. H. (1985b). Recent seismic reflection studies in Canada. *AGU Geophysical Series, Cornell Volume.* in press.

Jaeger, J. C.; and Cook, N. G. W. (1979). *Fundamentals of Rock Mechanics*, Fletcher & Sons Ltd, Norwich.

Kanamori, H. (1980). The state of stress in the Earth's lithosphere. in *Physics of the Earth's interior*, North-Holland Co.; 531–552.

--------(1983). Global seismicity. in *Earthquakes: Observation, Theory and Interpretation*, North-Holland Co.; 596–608.

Keen, C. E.; and Hyndman, R. D. (1979). Geophysical review of the continental of eastern and western Canada. *Canadian Journal of Earth Sciences* 16; 712-747.

Keilis-Borok, V. I.; and Malinovskaya, L. N. (1964). One regularity in the occurrence of strong earthquakes. *J. Geophys. Res.* 69; 3019-3024.

Keilis-Borok, V. I.; Knopoff, L.; Rovain, I. M.; and Sidorenko, T. M. (1980). Bursts of seismicity as long-term precursors of strong earthquakes. *J. Gwophys. Res.* 85; 813-820.

Kirby, S. H. (1977). State of stress in the lithosphere: Inference from flow laws of olivine. *Pure and Appl. Geophys.* 115; 245-258.

Lamoreaux, R. (1982). *Cluster Patterns in Seismicity*. Ph.D. Thesis, University of Alberta, Edmonton.

Landau, L. D.; and Lifshitz, E. M. (1959). *Theory of Elasticity*. Pergaman Press, Oxford, England; pp15.

Leed, D. K.; Kausel, E. G.; and Knopoff, L. (1974). Variations of upper mantle structure under the Pacific Ocean. *Science* 186; 141-143.

Lewis, T. (1985). A heat flux profile across southern Vancouver Island to the Garibaldi Volcanic Belt. personal communication.

McKenzie, D. P. (1969).Plate tectonic. in *The Nature of Solid Earth*, Robertson E. C., McGraw Hill; 323-360.

McMechan, G. A.; and Spence, G. D. (1983). P-wave velocity structure of the Earth's crust beneath Vancouver Island. *Canadian Journal of Earth Sciences* 20; 742-752.

Milne, W. G.; Rogers, G. C.; Riddihough, R. P.; McNechan G. A.; and Hyndman, R. D. (1978). Seismicity of Western of Canada. *Canadian Journal of Earth Sciences* 15; 1170–1193.

Monger, J. W. H.; Souther, J. G.; and Gabrielse, H. (1972). Evolution of the Canadian Cordillera: a plate-tectonic model. *American Journal of Science* 272; 577-602.

Muller, J. E. (1977). Evolution of the Pacific Margin, Vancouver Island, and adjacent region; *Canadian*

Journal of Earth Sciences 14, 2062-2085.

Riddihough, R. P. (1977). A model for recent plate interactions off Canada's west coast. *Canadian Journal of Earth Sciences*, 14; 384-396.

Richardson, R. M. (1978). Finite element modelling of stress in the Nasca plate: driving forces and plate boundary earthquakes; *Tectonophysics* 50; 223–248.

Riddihough, R. P. (1979) Gravity and structure of an active margin — British Columbia and Washington. *Canadian Journal of Earth Sciences* 16; 350–363.

Riddihough, R. P.; and Hyndman, R. D. (1976). Canada's active western margin—the case for subduction. *Geoscience Canada*, 3; 269-278.

Rogers, C. C. (1979). Earthquakes fault plane solutions near Vancouver Island. *Canadian Journal of Earth Sciences* 16; 523–531.

Shimazaki, K.; and Nakata, T. (1980). Time predictable recurrence model for large earthquakes. *Geophys. Res. Letter* 7; 279–282.

Silver, E. A. (1972). Pleistocene tectonic accretion of the continental slop off Washington. *Mstinr Geology*, 13;239-249.

Snavely, P. D.; and Wagner, H. C. (1981). Geological cross section across the continental margin off Vape Flattery, Washington, and Vancouver Island, British Columbia; *U. S. Geol. Surv. Open file Report* 81; 978-984.

Solomon, S. C.; Richardson, R. M.; and Bergman, E. A. (1980). Tectonic stress: models and magnitudes. *J. Geophys. Res.* 79; 6086–6092.

Stacey, F. D. (1977). *Physics of the Earth*, second edition. John Wiley & Sons, Inc. pp. 204.

------, (1977b). *Physics of the Earth*, second edition. John Wiley & Sons, Inc. pp. 296.

Stacey, R. A. (1973). Gravity anomalies, crustal structure, and plate tectonics in the Canadian Cordillera. *Canadian Journal of Earth Sciences* 10; 615–628.

Sweeney, J. F. (1985). Gravity measurements along the Vancouver Island Lithoprobe transect. personal communication.

Turcotte, D. L. (1974). Are transform faults thermal contraction cracks. *J. Geophys. Res*, 79; 2573-2677.

Uribe-Carvajal, A.; and Nyland, E. (1982) Elastic models of seismic failure in the Valley of Mexico. *Pure and Appl. Geophys.* 120, 1–13.

Uribe-Carvajal, A.; and Nyland, E. (1983) Evaluation of the risk of induced seismicity at the Itzantun hydroelectric site. Chiapas, Mexico. *Engineering Geology* 19, 247–259.

Uribe-Carvajal, A. (1984) *Seismic Stability Studies near the Middle America Trench.* Ph.D. thesis, University of Alberta, Edmonton.

Uribe-Carvajal, A.; and Nyland, E. (1985). Stochastic finite element calculation of seismic risk. *Tectonophysics* 117; in printing.

Von Henue, R.; and Kulm, L. D. (1973). Tectonic summary of Leg 18. *In* initial reports of the Deep Sea Drilling Project XVIII. U. S. Government Printing Office, Washington, D. C.; 961–976.

Watts, A. B.; Bodine, J. H.; and Steckler, M. S. (1980). Observations of flexure and the state of stress in the oceanic lithosphere. *J. Geophys. Res.* 85; 6369–6376.

Wiens, D. A.; and Stein, S. (1983). Age dependence of oceanic intraplate seismicity and implications for lithosphereic evolution. *J. Geophys. Res.* 88; 6456–6468.

Yole, R. W. (1969). Upper Paleozoic stratigraphy of Vancouver Island, British columbia. *Proceedings, Geological Association of Canada* 20; 30-40.

Yorath, R. M.; Clowes, R. M.; Brown, A. S.; Brandon, M. T.; Massey, N. W. D.; Green, A. G.; Spencer, C.; Kanasewich, E. R.; and Hydnman, R. D. (1984). Lithoprobe-Phase 1: Southern Vancouver Island: Preliminary analyses of reflection seismic profiles and surface geological studies. *Geological Survey of Canada Paper*; 85-1A, 543-554.

Appendix

The finite element technique is a powerful tool for calculating the stress field for a body with irregular boundaries and complex materials. This technique is used for the calculation of the stress field in this thesis. One of the difficulties in this technique is the tremendous amount of working time needed for preparing the input data file. Once the input data file is ready, it is time consuming to do any slight modification of the model. To overcome these problems an interactive graphics Fortran program was writen. This program can add or delete nodes or elements on the model, or move a node from one position to another. It can be used easily to vary the model and operates on the screen of a graphic terminal. The program is attached.

```
$R *FORTG
      DIMENSION X(1000),Y(1000),X1(10),X2(10)
     .    ,Y1(10),Y2(10),U(1000),V(1000),TH(1500)
      INTEGER*4 IELMS(3,1500),KNOD(1000),MAT(1500)
C
      CALL READIN(X,Y,NNODES,IELMS,NELMS,U,V,TH,MAT,KNOD)
C
      II=1
      CALL USMNMX(X,NNODES,1,XMIN,XMAX)
      CALL USMNMX(Y,NNODES,1,YMIN,YMAX)
      CALL WINDOW(XMIN,XMAX,YMIN,YMAX)
      X1(II)=XMIN
      X2(II)=XMAX
      Y1(II)=YMIN
      Y2(II)=YMAX
      CALL IGINIT
      CALL IGCTRL('TERM','SCREEN','SQUARE')
2     CALL IGBGNS('MODL')
      CALL IGCTRL('TERMINAL','ERASE')
      CALL IGTRAN('MODL','WIND',X1(II),X2(II),Y1(II),Y2(II))
      CALL IGBGNS('ELMS')
      CALL DRWLMS(X,Y,NNODES,IELMS,NELMS)
      CALL IGENDS('ELMS')
C     CALL IGBGNS('NODS')
C     CALL DRWNDS(X,Y,NNODES)
C     CALL IGENDS('NODS')
      CALL IGENDS('MODL')
C
      CALL IGBGNS('MENU')
      CALL MENU('BLOWUP<E>', -0.9,0.9)
      CALL MENU('BACK<E>', -.6,0.9)
      CALL MENU('STOP<E>',0.0,0.8)
      CALL MENU('ADDNODES<E>',0.3,0.9)
      CALL MENU('SUBNODES<E>',0.6,0.9)
      CALL MENU('ADDELEMS<E>',-0.9,0.8)
      CALL MENU('SUBELEMS<E>',-0.6,0.8)
      CALL MENU('WRITE<E>',-0.25,0.8)
      CALL MENU('REDRAW<E>',-0.3,0.9)
      CALL MENU('RDWO<E>',-0.0,0.9)
      CALL MENU('SCREEN DUMP<E>',0.2,0.8)
      CALL MENU('DRWNEWP<E>',0.63,0.8)
      CALL MENU('MVNOD<E>',-0.9,0.7)
      CALL IGENDS('MENU')
C
3     CALL IGCTRL('TERMINAL','ERASE')
      CALL IGCTRL('TERMINAL','KEEP',1)
1     CALL IGTRAN('MODL','WIND',X1(II),X2(II),Y1(II),Y2(II))
4     JUMP=IGPIKS('BLOW','BACK','STOP','ADDN','SUBN','ADDE','SUBE',
     &'WRIT','REDR','RDWO','SCRE','DRWN','MVNO')
      GOTO (1000,2000,3000,4000,5000,6000,7000,8000,9000,1100,
     .1200,1300,1400),JUMP
C
1000  PRINT 1001
1001  FORMAT('  ENTER LOWER LEFT CORNER')
      CALL IGXYIN(XLEFT,YLOWER)
      XLEFT=SCALE(XLEFT,X1(II),X2(II))
      YLOWER=SCALE(YLOWER,Y1(II),Y2(II))
      PRINT 1002
1002  FORMAT('  ENTER UPPER RIGHT CORNER')
      CALL IGXYIN(XRIGHT,YUPPER)
```

```
      XRIGHT=SCALE(XRIGHT,X1(II),X2(II))
      YUPPER=SCALE(YUPPER,Y1(II),Y2(II))
      CALL WINDOW(XLEFT,XRIGHT,YLOWER,YUPPER)
      X1(II+1)=XLEFT
      X2(II+1)=XRIGHT
      Y1(II+1)=YLOWER
      Y2(II+1)=YUPPER
      II=II+1
      GOTO 3
C
2000  II=II-1
      GOTO 3
4000  CALL ADDNOD(X,Y,NNODES,500,IELMS,NELMS,X1(II),X2(II),Y1(II)
     .,Y2(II),U,V,KNOD)
      GOTO 4
5000  CALL SUBNOD(X,Y,NNODES,IELMS,NELMS,X1(II),X2(II),Y1(II)
     .,Y2(II),U,V,KNOD)
      GOTO 4
6000  CALL ADDELM(X,Y,NNODES,IELMS,NELMS,1000,X1(II),X2(II),Y1(II),
     .Y2(II),TH,MAT)
      GOTO 4
7000  CALL SUBELM(X,Y,NNODES,IELMS,NELMS,X1(II),X2(II),Y1(II)
     .,Y2(II),TH,MAT)
      GOTO 4
8000  CALL WRIT1(X,Y,NNODES,IELMS,NELMS,U,V,TH,MAT,KNOD)
      GOTO 4
9000  GOTO 3
1100  II=1
      GOTO 3
1200  CALL IGDRON('CALC')
      GO TO 1
C
1300  GOTO 2
1400  CALL MVNOD(X,Y,NNODES,X1(II),X2(II),Y1(II),Y2(II))
      GOTO 1
3000  CALL IGCTRL('CALC','ENDPLOT')
      STOP
      END
C
      SUBROUTINE READIN(X,Y,NNODES,IELMS,NELMS,U,V,TH,MAT,KNOD)
      DIMENSION X(1000),Y(1000),U(1000),V(1000),TH(1500)
      INTEGER*4 IELMS(3,1500),MAT(1500),KNOD(1000)
      READ(5,100)NNODES,(N,KNOD(I),X(I),Y(I),U(I),V(I),I=1,NNODES)
100   FORMAT(I5//(I6,I6,2F12.2,2E12.2))
      READ(5,102)NELMS
      READ(5,103)(M,(IELMS(J,M),J=1,3),MAT(M),TH(M),M=1,NELMS)
102   FORMAT(I5)
103   FORMAT(I6,4I6,F6.1)
      RETURN
      END
C
      SUBROUTINE WINDOW(XMIN,XMAX,YMIN,YMAX)
      IF(YMAX-YMIN.GE.XMAX-XMIN) GOTO 1
      Y1=(YMAX+YMIN)/2-(XMAX-XMIN)/2
      Y2=(YMAX+YMIN)/2+(XMAX-XMIN)/2
      YMIN=Y1
      YMAX=Y2
      RETURN
1     X1=(XMAX+XMIN)/2-(YMAX-YMIN)/2
      X2=(XMAX+XMIN)/2+(YMAX-YMIN)/2
```

```
      XMIN=X1
      XMAX=X2
      RETURN
      END
C
      SUBROUTINE WRIT1(X,Y,NNODES,IELMS,NELMS,U,V,TH,MAT,KNOD)
      DIMENSION X(NNODES),Y(NNODES),U(NNODES),V(NNODES),TH(NELMS)
      INTEGER*4 IELMS(3,NELMS),MAT(NELMS),KNOD(NNODES)
      WRITE(7,100)NNODES,(I,KNOD(I),X(I),Y(I),U(I),V(I),I=1,NNODES)
100   FORMAT(I5/(2I6,4G12.2))
      WRITE(7,200)NELMS
      WRITE(7,300)(M,(IELMS(J,M),J=1,3),MAT(M),TH(M),M=1,NELMS)
200   FORMAT(I5)
300   FORMAT(5I6,F6.0)
      RETURN
      END
C
      SUBROUTINE MENU(STRING,X,Y)
      DIMENSION STRING(1)
      CALL IGBGNS(STRING)
      CALL IGMA(X,Y)
      CALL IGTXT(STRING)
      CALL IGENDS(STRING)
      RETURN
      END
C
      SUBROUTINE DRWLMS(X,Y,NNODES,IELMS,NELMS)
      REAL*4 X(NNODES),Y(NNODES),XE(4),YE(4)
      INTEGER*4 IELMS(3,NELMS)
      DO 1 I=1,NELMS
      DO 2 J=1,3
      XE(J)=X(IELMS(J,I))
2     YE(J)=Y(IELMS(J,I))
      XE(4)=X(IELMS(1,I))
      YE(4)=Y(IELMS(1,I))
1     CALL IGVEC(4,XE,YE)
      RETURN
      END
C
      FUNCTION SCALE(S,X1,X2)
      SCALE=S*(X2-X1)/2.+(X2+X1)/2.
      RETURN
      END
C
      INTEGER FUNCTION PIKNOD(X,Y,NNODES,X1,X2,Y1,Y2)
      REAL*4 X(NNODES),Y(NNODES)
      CALL IGXYIN(XIN,YIN)
      XIN=SCALE(XIN,X1,X2)
      YIN=SCALE(YIN,Y1,Y2)
      DIST=(X(1)-XIN)**2+(Y(1)-YIN)**2
      PIKNOD=1
      DO 1 I=1,NNODES
      DST=(X(I)-XIN)**2+(Y(I)-YIN)**2
      IF(DST.GE.DIST)GO TO 1
      DIST=DST
      PIKNOD=I
1     CONTINUE
      WRITE(6,222)PIKNOD
222   FORMAT('NODE',I8)
      RETURN
```

```
      END
C
      SUBROUTINE DRWNDS(X,Y,NNODES)
      REAL*4 X(NNODES),Y(NNODES)
      DO 1 I=1,NNODES
      CALL IGMA(X(I),Y(I))
1     CALL IGSYM('W')
      RETURN
      END
C
      SUBROUTINE ADDNOD(X,Y,NNODES,NMAX,IELMS,NELMS,X1,X2,Y1,Y2
     .,U,V,KNOD)
      REAL*4 X(NMAX),Y(NMAX),U(NMAX),V(NMAX)
      INTEGER*4 IELMS(3,NELMS),PIKNOD,KNOD(NMAX)
      IF(NNODES.LT.NMAX) GOTO 5
      CALL UERTST(33,'ADDNOD')
      RETURN
5     PRINT 100
100   FORMAT(' PICK A NODE AFTER WHICH YOU WILL ADD A NEW NODE')
      NTEMP=PIKNOD(X,Y,NNODES,X1,X2,Y1,Y2)
      NT=NNODES-NTEMP
      DO 2 I=1,NT
      Y(NNODES+2-I)=Y(NNODES+1-I)
      X(NNODES+2-I)=X(NNODES+1-I)
      U(NNODES+2-I)=U(NNODES+1-I)
      V(NNODES+2-I)=V(NNODES+1-I)
2     KNOD(NNODES+2-I)=KNOD(NNODES+1-I)
      PRINT 101
101   FORMAT(' ADD THE NEW NODES')
      CALL IGXYIN(XX,YY)
      X(NTEMP+1)=SCALE(XX,X1,X2)
      Y(NTEMP+1)=SCALE(YY,Y1,Y2)
      NNODES=NNODES+1
      CALL ARRE(IELMS,NELMS,NTEMP+1,1)
      PRINT 102
102   FORMAT('DO YOU WANT TO SPECIFY B.C. ?'/
     . '   1=YES,0=NO')
      READ(6,103)K
103   FORMAT(I1)
      IF(K.EQ.1)GOTO 3
      U(NTEMP+1)=0.0
      V(NTEMP+1)=0.0
      KNOD(NTEMP+1)=0
      GOTO 4
3     PRINT 104
104   FORMAT('INPUT CODE OF B.C. (KNOD=?) ')
      READ(6,105)L
105   FORMAT(I2)
      KNOD(NTEMP+1)=L
      PRINT 106
106   FORMAT('INPUT U AND V')
      READ(6,107)UU,VV
107   FORMAT(2G12.2)
      U(NTEMP+1)=UU
      V(NTEMP+1)=VV
4     CALL IGMA(XX,YY)
      CALL IGTXT('+<E>')
      RETURN
      END
C
```

```
      SUBROUTINE SUBNOD(X,Y,NNODES,IELMS,NELMS,X1,X2,Y1,Y2,
     . U,V,KNOD)
      REAL*4 X(NNODES),Y(NNODES),U(NNODES),V(NNODES)
      INTEGER*4 IELMS(3,NELMS),PIKNOD,KNOD(NNODES)
      PRINT 100
100   FORMAT(' WHICH NODE YOU WANT TO SUBTRACT')
      INDEX=PIKNOD(X,Y,NNODES,X1,X2,Y1,Y2)
      NLMS=NELMS
      DO 1 I=1,NELMS
      DO 2 J=1,3
      IF(IELMS(J,I).NE.INDEX)GO TO 2
      NLMS=NLMS-1
      DO 3 K=I,NLMS
      DO 3 L=1,3
3     IELMS(L,K)=IELMS(L,K+1)
      J=3
      I=I-1
2     CONTINUE
      IF(I.GE.NLMS)I=NELMS+1
1     CONTINUE
      NELMS=NLMS
      NNODES=NNODES-1
      DO 4 I=INDEX,NNODES
      X(I)=X(I+1)
      Y(I)=Y(I+1)
      U(I)=U(I+1)
      V(I)=V(I+1)
4     KNOD(I)=KNOD(I+1)
      CALL ARRE(IELMS,NELMS,INDEX,-1)
      RETURN
      END
C
      SUBROUTINE ARRE(IELMS,NELMS,INDEX,NSIGN)
      INTEGER*4 IELMS(3,NELMS)
      DO 1 I=1,NELMS
      DO 1 J=1,3
      IF(IELMS(J,I).LT.INDEX) GOTO 1
      IELMS(J,I)=IELMS(J,I)+NSIGN
1     CONTINUE
      RETURN
      END
C
      INTEGER FUNCTION PIKELM(X,Y,NNODES,IELMS,NELMS,X1,X2,Y1,Y2)
      REAL*4 X(NNODES),Y(NNODES)
      INTEGER*4 IELMS(3,NELMS),II(3),PIKNOD
      PRINT 100
100   FORMAT(' INPUT THREE NODES OF THE ELEMENT')
      DO 5 I=1,3
      II(I)=PIKNOD(X,Y,NNODES,X1,X2,Y1,Y2)
5     PRINT 101
101   FORMAT('OK')
      DO 1 I=1,NELMS
      DO 2 J=1,3
      DO 3 K=1,3
      IF(IELMS(J,I).EQ.II(K))GO TO 2
3     CONTINUE
      GOTO 1
2     CONTINUE
      PIKELM=I
      RETURN
```

```
1     CONTINUE
      PIKELM=-1
      RETURN
      END
C
      SUBROUTINE ADDELM(X,Y,NNODES,IELMS,NELMS,NEMAX,X1,X2,Y1,Y2,TH,MAT)
      REAL*4 X(NNODES),Y(NNODES),TH(NEMAX)
      INTEGER*4 IELMS(3,NEMAX),PIKNOD,PIKELM,MAT(NEMAX)
      IF(NELMS.LT.NEMAX)GOTO 1
      CALL UERTST(33,'ADDELM')
      RETURN
1     PRINT 100
100   FORMAT(' PICK A ELEMENT AFTER WHICH YOU WILL ADD A NEW ONE')
      INDEX=PIKELM(X,Y,NNODES,IELMS,NELMS,X1,X2,Y1,Y2)
      NT=NELMS-INDEX
      DO 2 I=1,NT
      DO 2 J=1,3
2     IELMS(J,NELMS+2-I)=IELMS(J,NELMS+1-I)
      NELMS=NELMS+1
      PRINT 101
101   FORMAT(' ADD NEW ELEMENT, INPUT THREE NODES IN ORDER OF COUNTERCLO
     &CKWISE')
      DO 5 I=1,3
      IELMS(I,INDEX+1)=PIKNOD(X,Y,NNODES,X1,X2,Y1,Y2)
5     PRINT 102
102   FORMAT('OK')
      PRINT 103
103   FORMAT('INPUT CODE OF MATERIAL AND THIKNESS, (MAT & TH) '/
     .'INPUT 0.0 FOR UNIT THIKNESS')
      READ(6,104)MM,TT
104   FORMAT(I2,F6.0)
      MAT(INDEX+1)=MM
      TH(INDEX+1)=TT
      RETURN
      END
C
      SUBROUTINE SUBELM(X,Y,NNODES,IELMS,NELMS,X1,X2,Y1,Y2,TH,MAT)
      REAL*4 X(NNODES),Y(NNODES),TH(NELMS)
      INTEGER*4 IELMS(3,NELMS),PIKELM,MAT(NELMS)
      PRINT 100
100   FORMAT(' PICK A ELEMENT YOU WANT TO SUBTRACT')
      INDEX=PIKELM(X,Y,NNODES,IELMS,NELMS,X1,X2,Y1,Y2)
      DO 1 I=INDEX,NELMS
      TH(I)=TH(I+1)
      MAT(I)=MAT(I+1)
      DO 1 J=1,3
1     IELMS(J,I)=IELMS(J,I+1)
      NELMS=NELMS-1
      RETURN
      END
C
      SUBROUTINE MVNOD(X,Y,NNODES,X1,X2,Y1,Y2)
      REAL*4 X(NNODES),Y(NNODES)
      INTEGER PIKNOD
      PRINT 100
100   FORMAT('PICK UP THE NODE')
      INDEX=PIKNOD(X,Y,NNODES,X1,X2,Y1,Y2)
      PRINT 101
101   FORMAT('INPUT NEW COORDINATE')
      CALL IGXYIN(XIN,YIN)
```

```
      X(INDEX)=SCALE(XIN,X1,X2)
      Y(INDEX)=SCALE(YIN,Y1,Y2)
      RETURN
      END
$ENDFILE
$IF RC>0 $SOU PREVIOUS
$R -LOAD#+*IG+*IMSLLIB 5=m2p1 4=DSTRESS 9=-P 7=-F
$EXEC *ESPPRUN -P FEET=20 RETURN=PHYS
```